Stable Isotope Systematics of Fluids and Epidote~~s~~ in the Bacon-Manito Geothermal Field, Philippines: Indicators of Fluid Origin and Evolution

Julius John T. Dimabayao[a], Michael C. Rowe[b*], and Shaun Barker[c]

[a]*Energy Development Corporation – Bacman Geothermal Business Unit, Legazpi City, Philippines*
[b]*School of Environment, The University of Auckland, Auckland, New Zealand*
[c]*Centre for Ore Deposits and Earth Science, University of Tasmania, Hobart, Australia*

Keywords: hydrogen stable isotopes; hydrothermal epidote; magmatic arc geothermal systems; oxygen stable isotopes; renewable energy

* Corresponding author at: University of Auckland, School of Environment, 23 Symonds St, 1142 Auckland. +64 9 9236682, michael.rowe@auckland.ac.nz

Abstract

The physiochemical evolution of active geothermal systems is important for assessing their long-term viability. Although discharge fluid chemistry provides information on geothermal well conditions, it only typically reflects the current state of the reservoir. Integration of fluid chemistry with rock and mineral chemistry can fill this gap by providing a longer-term record of fluctuations in geothermal conditions. This study examines the stable isotope systematics and the hydrogeological model of the Bacon-Manito geothermal field (Bacman) in the Philippines, a liquid-dominated, volcanic field-type geothermal system in a convergent setting. ~~Geochemical data from geothermal~~ Geo~~t~~thermal well discharge geochemistry~~s~~ is~~are~~ supported~~lemented with~~ by hydrogen and oxygen isotope data and elemental composition data from hydrothermal epidote~~s~~ and reservoir rocks. Chemical and isotopic analyses of well discharges reveal~~s~~ short-term processes that are affecting the Bacman reservoir from the onset of fluid extraction due to field operations. Boiling within the Botong sector and the incursion of peripheral and injection fluids into the main reservoir of Palayang Bayan and Cawayan sectors was~~ere~~ observed from the changes in isotopic and chemical compositions of well discharges. Meanwhile, changes in epidote morphology and associated mineral assemblages, as well as epidote $\delta^{18}O$ ~~values and mineral chemistry~~major-element compositions, are related~~closely linked~~ to reservoir rock composition, fluid chemistry, and temperature. These factors dictate the extent to which water-rock interaction

and fluid mixing, the two most prominent processes in the isotopic evolution of epidote~~s~~ and fluids in Bacman, affect each particular sector in the reservoir.

We present ~~here~~ an updated and expanded hydrogeological model of Bacman by incorporating the exploration sectors of Rangas and Kayabon. A heat source associated with carbonate reservoir rocks is postulated for the Rangas sector. ~~The presence of carbonate host rocks in Rangas and a postulated heat source would suggest that water-rock interaction is a dominant process.~~ Fluids in the Rangas~~is~~ sector originated from the main reservoir upflow in Botong and are~~were~~ isotopically enriched through interaction with carbonate reservoir rocks, suggesting that water-rock interaction is the dominant process. In contrast, the existence of fluids with ~~varying~~ variable isotopic compositions in the Palayan Bayan and Cawayan sectors ~~would naturally drive~~indicates ~~varying degrees of fluid mixing as the~~ ~~a dominant process~~. The present-day fluids~~,~~ evolved through the continuous mixing of isotopically enriched parent waters with isotopically depleted peripheral waters. Further, fluids and epidotes from Kayabon are~~were~~ found to be isotopically and petrologically distinct from the rest of the Bacman reservoir, ~~further suggesting that~~supporting a relatively cooler and waning heat source ~~exists~~ beneath the sector.

1. Introduction

The Philippines is currently the world's second largest producer of geothermal energy for power production (Bertani, 2015). The country's geological setting as an island arc in the Western Pacific is ideal for the development of Quaternary and ~~R~~recent volcanism-related high-temperature geothermal systems (Sussman et al., 1993). In line with efforts to increase power production, exploration of frontier areas and development of existing geothermal systems in the country call for a better understanding of how fluids evolve in these magmatic-driven hydrothermal systems. Stable isotopes are particularly important for constraining fluid evolution. Pioneering studies of stable isotopes (e.g., Craig, 1963) have enabled their application to geothermal systems as natural tracers to determine the origin and evolution of these fluids. Stable isotopes also help determine reservoir processes, such as meteoric-magmatic fluid mixing and water-rock interaction, which~~that~~ may ~~have~~ ~~a~~affect~~ed~~ the fluid composition ~~of these fluids~~.

While ~~fluid~~ the chemistry ~~may record~~of modern hydrothermal fluids provides evidence on the current conditions of a geothermal field, it is also important to look at the rock record, in particular the alteration mineralogy, to understand past conditions and the evolution of the entire system. Epidote is a common ~~and geologically important~~ alteration mineral associated with water-rock interaction in hydrothermal systems (Bird and Spieler, 2004). Hydrogen, oxygen, and chlorine isotopes are among the most suitable for studying the isotope systematics of epidote due to their abundances in epidote and relation to fluid chemistry (Morrison, 2004). H and O isotopes are the more extensively investigated, primarily because of lower Cl abundances in minerals and fluids (Frei et al., 2004). The fractionation factor of $^{18}O/^{16}O$ and D/H between epidote minerals and water has been the subject of many ~~works~~ prior studies (e.g., Zheng, 1993 for O isotopes and Chacko et al., 1999 for H isotopes). Furthermore, these works also determined the effects of temperature o~~i~~n the isotope fractionation of $^{18}O/^{16}O$ (Matsuhisa et al., 1979; Matthews et al., 1983; Kohn and Valley, 1998) and D/H (Graham and Sheppard, 1980; Graham et al., 1980; Vennemann and O'Neil, 1996; Chacko et al., 1999) between various epidote group minerals and water through experimental studies ~~through empirical studies~~. These works paved the way for the application of stable isotopes in a variety of studies (e.g., Zen and Hammarstrom, 1984; Bird et al., 1988; and Cartwright et al., 1996) concerned with determining hydrothermal fluid sources that are involved in the formation of epidote minerals. The range of epidote-hosted systems~~s~~ examined in these studies includes metamorphic environments, deep-seated plutons, and hydrothermal systems (Morrison, 2004).

In this study, we focus on investigating the chemical and isotopic composition of geothermal fluids and hydrothermal epidote~~s~~ in the Bacon-Manito geothermal field (Bacman), Philippines. The primary objectives are to determine the spatio-temporal evolution of hydrothermal fluids in the field, ~~give light on the~~illuminate processes involved in the changes ~~in the nature of~~to the reservoir, and formulate an updated model for the field, which now includes potential sectors for expansion. Although there have been comprehensive studies on the isotopic composition of Bacman geothermal fluids as natural tracers (e.g., Ruaya et al., 1993; Martinez-Olivar et al., 2005), corresponding geochemical studies from reservoir rocks and minerals are lacking in the literature. Thus, reservoir processes and changes, ~~which are~~better recorded ~~better~~ by rock and mineral samples, are largely overlooked. This gap highlights the limitation ~~of~~ for understanding the nature

of a geothermal reservoir when ~~only~~ looking at ~~datasets from~~ liquid-only ~~samples~~datasets. Isotopic compositions of hydrothermal epidote~~s~~ from selected reservoir rocks in Bacman provide additional perspective on the stable isotope systematics of the field. Pope et al. (2014, 2016) stressed the importance of isotope data from water-bearing hydrothermal minerals to complement isotope data from geothermal well discharges. These ~~works~~ investigations utilized both $^{18}O/^{16}O$ and D/H stable isotopes ~~records~~ from hydrothermal epidote~~s~~ in the rift-hosted Reykjanes and Krafla Icelandic geothermal fields~~, both of which are rift-hosted geothermal systems in Iceland~~. Following the methodology of Pope et al. (2014, 2016), we utilize a holistic geochemical approach ~~combination of fluid, rock, and mineral chemistry~~ to evaluate the origin of hydrothermal fluids, and illustrate ~~different~~ water-rock interactions ~~processes~~ that contributed to the evolution of these fluids, for the magmatic arc-driven Bacman geothermal system.

2. Geologic Background

The Bacman geothermal field is located in the Pocdol Mountains, Philippines, a cluster of ~~eruptive~~ volcanic centers ~~that are dated~~erupted between 6.4 Ma and 0.04 Ma (Bruinsma, 1983; Tebar, 1988; JICA, 1999; Ozawa et al., 2004) and scattered on a rugged topography that is part of the Bicol volcanic arc ~~system in~~on the Bicol peninsula, Luzon Island (Fig. 1). These volcanic complexes are the outcome of ~~the~~ active subduction of the Philippine Sea Plate, resulting in young volcanism and emplacement of volcanic ~~deposits on top of~~material overlying sedimentary ~~units~~, metamorphic, and ophiolitic basement lithologies ~~complexes~~ in the Bicol basin (Andal et al., 2005; DENR-MGB, 2004). This type of setting provides active heat sources for volcanic field-type geothermal systems to develop (Moeck, 2014). Currently, the geothermal producing areas in Bacman are located in the Palayang Bayan, Cawayan and Botong sectors, while potential ~~sectors for~~ expansion includes the Tanawon, Rangas and Kayabon sectors (Villacorte et al., 2015).

~~Hydrothermal alteration and fluid chemistry of Bacman have been the subject of many different pioneering studies~~Pioneering studies of hydrothermal alteration and fluid chemistry within the Bacman geothermal field have served as a foundation for the development of conceptual models of the Bacman reservoir (e.g., Lawless et al., 1983; Panem and Alincastre, 1985; Reyes, 1985; Tebar, 1988; Ruaya et al., 1993 and D'Amore et al., 1993). ~~These works have been the foundation of subsequent studies that allowed for the development of conceptual models of the Bacman~~

~~reservoir.~~ Surface investigations and drilling in Bacman ~~showed~~ have shown a predominant hydrothermal alteration assemblage ~~from f~~that formed in equilibrium with ~~luid-rock interaction with~~ neutral-~~-~~pH fluids, along with minor alteration assemblages associated with~~due to presence of~~ shallow acidic fluids (Lawless et al., 1983; Reyes, 1985). The intensity and grade of alteration (respectively defined as the abundance of alteration minerals in a rock, and the ~~type of~~temperature-dependent mineral assemblage~~ depending on temperature~~) vary in different lithologies. The lower inherent permeability of the ~~volcanic rocks compared to~~ deeper sedimentary and intrusive rocks compared to overlying volcanic rocks (Zaide-Delfin et al., 1989) contributes to their lower degree of alteration, evidenced by sectional isotherms based on alteration mineralogy (Ramos and Santos, 2012). ~~are mostly intensely altered (Ramos and Santos, 2012), while sedimentary and intrusive rocks were observed to be less altered (Zaide-Delfin et al., 1989). Hydrothermal mineralogy in~~In the predominantly porphyritic andesite host rocks, alteration can form~~s both~~ from replacement of original minerals and/or from vein minerals infilling fractures (Santos, 2014).

~~Mineral~~ Host-rock alteration mineral assemblages ~~due to interaction of host rocks with~~associated with dilute neutral-pH fluids are ~~found almost throughout~~extensive in the deeper portion of the Bacman reservoir. These ~~can be classified into~~reservoir temperature-dependent mineral suites ~~with occurrences that are strongly dependent on reservoir temperature, and thus~~ are utilized as geothermometers during drilling (Reyes, 1985). Low temperature (< 180 °C to 220 °C) minerals include silica phases (cristobalite, opal, tridymite), chlorite, laumontite and clays such as smectite and illite-smectite. High temperature (220 °C to > 300 °C) minerals include illite, epidote, wairakite, tremolite-actinolite and secondary biotite. Along with available fluid inclusion data, these minerals provide ~~information on the~~ reservoir temperature variation across the field (Ramos and Santos, 2012).

Hydrothermal epidote~~s~~ ~~are~~ is a common alteration mineral~~s~~ in assemblages from dilute, neutral-pH fluid~~-~~ and rock interaction. The stability and mineral morphology ~~of the mineral~~ is~~are~~ highly dependent on ~~formation~~ temperature (Keith et al., 1968; Patrier et al., 1990), permeability and fluid composition~~ (Arnason and Bird, 1992)~~, ~~as well as~~including silica activity and CO_2 fugacity (Giggenbach, 1984; Arnason and Bird, 1992). In Bacman and other geothermal fields in the Philippines, epidote is particularly important during geothermal well drilling, as the onset of subhedral epidote in drill~~the~~ cuttings indicates ~~that the~~ a formation temperature ~~of the formation~~

~~can be~~ estimated at ~~around~~ 220 °C, the minimum temperature required for setting the production casing shoe of the well (Reyes, 1990). Macroscopically, epidote occurs in euhedral prisms or aggregates, and may form~~.~~ ~~It can be present~~ in veins or vugs, or ~~as a replacement mineral for~~replacing plagioclase, pyroxene, and hornblende (Santos, 2014).

~~Reservoir~~ Bacman reservoir fluid chemistry ~~data enabled the establishment of~~established a baseline ~~fluid chemistry~~ (Ruaya et al., 1993) prior to the full-blown fluid extraction of the field, revealing a~~.~~ ~~These data reveal that~~ dilute chloride fluid~~s~~ ~~exist~~ in the Bacman reservoir (D'Amore et al., 1993; Abrigo et al., 2006). The calculated maximum reservoir temperatures ~~based on the~~from quartz geothermometry~~er~~ (T_{quartz}) (Fouriner, 1977) ~~reach more than~~exceeds 300˚C in the upflow portion of the reservoir in the Botong sector, and temperatures gradually decrease towards the Palayang Bayan sector and ~~and further~~ to ~~the outflow in the northwest~~the northwest in the direction of the outflow. Reservoir chloride (Cl_{res}) ~~) data also display a similar trend~~abundances similarly vary, reaching more than 8,000 mg/kg in the ~~from~~ Botong sector and decreasing to ~6,500 mg/kg in the Palayang Bayan sector (Ruaya et al., 1993; D'Amore et al., 1993).

3. Methods

3.1 Fluid Data and Reduction

~~Geochemical data for~~ Ggeothermal well fluid geochemistry~~s~~ was~~ere~~ obtained from Ruaya et al. (1993) and the Energy Development Corporation (EDC). Sampling and analytical procedures to obtain chemical and isotopic parameters were~~are~~ ~~laid out~~ conducted in accordance to sampling methods and standards as described by Arnórsson and IAEA (2000). Reservoir fluid compositions were calculated ~~Liquid data reduction was done using~~following the methods ~~and calculations~~ developed by Fournier and Truesdell (1974) and revised by subsequent authors (e.g. Arnórsson, and IAEA, 2000, and Horita and Wesolowski, 1994)~~ to recalculate the reservoir fluid compositions~~.

Reservoir fluid compositions~~hemistry~~ may be modified by physical processes (e.g., phase separation, adiabatic boiling, and depressurization) during ~~flow through well bores~~transport towards the surface. Back-c~~C~~alculating ~~back~~ to ~~these values~~reservoir compositions requires data on separation pressure and discharge enthalpy (H) for each well during sampling. ~~These data are~~These variables are used to~~in~~ determine~~ning~~ the total discharge (C_{TD}) and reservoir (C_{res}) concentrations, which are then used to calculate the concentration of species in the reservoir from initial measurements ~~through data reduction when given initial laboratory results~~. C_{TD} is the recalculated composition of ~~a~~ the fluid component at the wellhead based on H (Equation 1), while C_{res} is the recalculated composition of the subsurface~~a~~ fluid component assumed to represent the initial reservoir fluid ~~in the subsurface and is assumed as the original concentration of the fluid component in the reservoir~~ (Equation 4).

$$C_{TD} = (1-y)\, C_l + yC_v \qquad \text{(Equation 1)}$$

where C_{TD} = total discharge concentration
C_l = concentration at liquid phase as analys~~z~~ed ~~in the lab~~
C_v = concentration at vapor phase as analys~~z~~ed ~~in the lab~~

and y is the steam fraction derived from PEPSE steam tables software (Scientech, 2005), expressed as

$$y = (H-h_f)/h_{fg} \qquad \text{(Equation 1.1)}$$

where h_f = specific enthalpy of liquid water at a given saturation pressure, as determined from steam tables
h_{fg} = specific enthalpy change of evaporation at a given saturation pressure, as determined from steam tables.

For components that are strongly soluble in the liquid phase ~~and~~ (i.e. do not partition ~~to vapor~~into the vapor phase), Equation 1 can be simplified as

$$C_{TD} = (1-y)\, C_l \qquad \text{(Equation 2)}$$

Geothermometers are utilized to determine ~~To determine their~~ C_{res}~~, chemical geothermometers may be utilized~~. Due to the empirically-defined relationships of their solubility-dependent reactions with temperature, chemical geothermometers (such as the quartz geothermometer, T_{quartz}, which considers waters in equilibrium with quartz after adiabatic boiling; ~~(~~Fournier, 1977~~)~~), are

used to recalculate the concentrations of cations and anions in the reservoir given the ~~original laboratory~~measured concentrations~~ values~~ (C) (Equation 3).

$$T_{quartz} = 1522 / (5.75 - \log C) - 273.15 \qquad \text{(Equation 3)}$$

Equations 3 and 4 assume two things: (1) fluids from the well must come from a single feed zone and, (2) ~~-~~no flashing has occurred within the wellbore to alter ~~altered~~ the original fluid composition. The latter can be tested by determining if there is an "excess enthalpy," wherein the discharge enthalpy (H) is much greater than the enthalpy of the saturated liquid fraction at the wellhead, which is usually based on T_{quartz} ($H_{Tquartz}$) (i.e., $H >> H_{Tquartz}$). If there is no excess enthalpy, then the calculated C_{TD} is assumed ~~as~~ to be equivalent to C_{res}~~the reservoir concentration~~. Otherwise, C_{res} ~~reservoir concentration~~ must be calculated using the steam fraction (y) obtained from $H_{Tquartz}$.

$$C_{res} = C\,[1- ((H_{Tquartz} - h_f) / h_{fg})] \qquad \text{(Equation 4)}$$

Similarly, isotopic data ~~must be~~are ~~reduced~~ recalculated to total discharge and reservoir values. ~~δ values refer to isotopic~~ Isotopic ratios ~~of~~ δD and δ~~D/H and~~ ^{18}O~~/^{16}O,~~ ~~which~~ are relative to ~~the~~ V-SMOW ~~standard~~ (Craig, 1961). ~~Due~~ As ~~to~~ ^{18}O and D partition~~ing~~ into both the liquid and vapor phases, calculation of δ_{TD} and δ_{res} compositions consider both the liquid and steam condensate samples.

$$\delta_{TD} = [(1-y)\,\delta_l] + y\delta_v \qquad \text{(Equation 5)}$$

where δ_l = isotopic composition at liquid phase as ~~analyzed~~analysed ~~in the lab~~
δ_v = isotopic composition of steam condensate as ~~analyzed~~analysed ~~in the lab~~

$$\delta_{res} = \delta_{TD} + [((H_{Tquartz} - h_f)/h_{fg})\ 10^3 \ln\alpha] \qquad \text{(Equation 6)}$$

where ~~$10^3 \ln\alpha$~~ liquid-vapor fractionation for D and ^{18}O based on T_{quartz} is derived from ~~the~~ Equations 7 and 8 as regressed by Horita and Wesolowski (1994).

$$10^3 \ln\alpha_{l\text{-}v}\,(D) = 1158.8\,(T^3/10^9) - 1620.1(T^2/10^6) + 794.84\,(T/10^3) - 161.04 + 2.9992(10^9/T^3)$$

(Equation 7)

$$10^3 \ln\alpha_{l\text{-}v}\,(^{18}O) = -7.685 + 6.7123(10^3/T) - 1.6664(10^6/T^2) + 0.35041(10^9/T^3) \qquad \text{(Equation 8)}$$

3.2 Rock sampling and analysis

Rock and mineral samples were gathered from borehole cuttings and available cores from selected sampling depths ranging from 1600 m to 2700 m, in four geothermal wells. These wells were selected to achieve optimal representation ~~of different sections of~~across the geothermal field. Borehole cuttings with appreciable epidote alteration from four wells (PAL18D and PAL30D from the Palayang Bayan sector, RS1D from the Rangas sector, and PAL8RD from the Kayabon sector; Fig. 1) were retrieved from the reservoir. For well PAL8RD, a new well ~~without much~~lacking comprehensive reservoir and fluid discharge data, whole rock major element compositions were measured by X-ray fluorescence (XRF) analysi~~e~~s at the University of Auckland ~~were also performed~~ on a PANalytical Axios XRF spectrometer for~~on~~ select~~ed~~ samples. ~~However~~ However~~unfortunately~~, XRF data is unavailable for the other three wells.~~.~~ Loss on ignition (LOI) ~~determination~~ was conducted on all sample powders ~~by~~ after heating ~~them~~ at 900 °C for 16 hours. Glass beads for XRF analysis, made from a 2:1 mixture by mass of non-ignited powder and lithium meta (64.7%)/ tetra (36.3%) borate, were fused in a PANalytical Eagon 2 at 1000 °C for 85 minutes. ~~Compositions were determined on a PANalytical Axios XRF spectrometer with~~ ~~r~~Reproducibility for major elements is~~of~~ ~~<~~ better than 0.1 wt%. Results of the whole rock XRF analyses are provided in Supplemental Table 2.

Alteration mineralogy was described semi-quantitatively ~~by taking note~~from observations of alteration intensity~~ and abundance of alteration minerals~~. The cuttings were further ground to a maximum diameter of~~ at most~~ ~1-2 mm to dislodge epidote crystals from other minerals and~~ the~~ groundmass. ~~Grains~~ Epidote grains that were ~~large enough (~~at least 0.2 mm in length~~)~~, ~~did not have~~and lacked altered rims, visible inclusions, or other attached minerals, were hand-picked ~~from the rest of the sample using~~under a binocular microscope. Following mineral separation, $^{18}O/^{16}O$, D/H isotopic analysis and electron microprobe analysis (EMPA) were performed on the epidote grains.

Epidote major- and minor-element abundances ~~Major and minor element compositions of epidote~~ (Si, Ca, Al, Fe, Mg, Mn, Ti, Ca, and Cr) were determined using electron microprobe analysis (EMPA) at Victoria University of Wellington on a JEOL 8230 'Superprobe'. Epidote~~s~~ was~~ere~~ analysed using a 12 nA, 15 kV focused electron beam. Internal standards Biotite-110 and Engels Hornblende were ~~used~~ analysed ~~as a check of~~to monitor accuracy and precision, independent of

calibration standards. ~~Results of the EMPA~~Epidote compositions are presented in Table 2. To ensure data quality, results were cross-referenced with epidote compositions from different sources (E.g. Shikazono, 1984; Bird et al., 1988, and Arnason et al., 1993) and checked stoichiometrically.

Epidote stable isotope compositions was measured by the GNS Isotope Laboratory in Lower Hutt, New Zealand. For D/H analysis, samples were analysed in triplicate using a HEKAtech high temperature elemental analyser coupled with a GV Instruments IsoPrime mass spectrometer. All results are reported with respect to V-SMOW, normalized to international standards IAEA-CH-7, NBS30 and NBS22 with reported δD values of -100‰, -66‰ and -118‰, and waters USGS46, 47, 48, and W62001 (-235.8‰, -150.2‰, -2.0‰, and -41.1‰, respectively). The external precision ~~for these measurements~~ is better than 2‰. For $^{18}O/^{16}O$ analysis, oxygen extraction was ~~done first using~~on a CO_2-laser and BrF_5-laser ablation line following the methods of Sharp (1990). Samples were ~~then~~ analys~~z~~ed using a Geo20-20 mass spectrometer with~~. Sample~~ results ~~were~~ normalized to NBS-28 (+9.6‰), with reproducibility, based on replication of NBS-28 (N=4), at < 0.15‰. I~~The results of i~~sotopic ~~analysis~~ results are expressed in delta notation relative to V-SMOW (‰). Epidote-fluid ~~The~~ fractionation factors ($10^3\ln\alpha$) ~~between epidote and water~~ for both D/H and $^{18}O/^{16}O$ were determined using Equation 9 following O'Neil (1986).

$$10^3\ln\alpha = 10^3\ln(1000 + \delta_{epidote} / 1000 + \delta_{fluid\cancel{water}}) \approx \delta_{epidote} - \delta_{fluid} \qquad \text{(Equation 9)}$$

T~~The t~~emperatures for~~on~~ specific sample depths were obtained from well temperature-depth profiles provided by EDC. T~~o calculate t~~he δD and $\delta^{18}O$ isotopic composition of fluids in equilibrium with epidote were calculated using ~~,~~ Equation~~s~~ 10 (Chacko et al., 1999) and 11 (Pope et al., 2016; as derived from the results of Matsuhisa et al., 1979; Matthews et al., 1983; and Kohn and Valley, 1998), ~~were used~~ following the procedure of Pope et al. (2016).

$$10^3\ln\alpha D_{epidote\text{-}fluid} = 9.3000\ (10^6/T^2) - 61.90 \qquad \text{(Equation 10)}$$

$$10^3\ln\alpha^{18}O_{epidote\text{-}fluid} = 1.53\ (10^6/T^2) - 3.31 \qquad \text{(Equation 11)}$$

A comparison between Equation 11 and fractionation curves derived by Zheng (1993) and Matthews et al. (1983) indicates a close approximation between these approaches (within ~2‰), and choice in the fractionation equation does not produce a significant effect on calculated results.

4. Results

4.1. Petrography and whole rock chemistry

Petrographic ~~data~~ observations from the four wells show a ~~predominant~~propylitic~~ly~~ ~~neutral and propylitic~~ alteration mineralogy of ~~(~~illite + chlorite + epidote + tremolite/actinolite,~~)~~ as a result of host rock interaction with dilute neutral-pH fluids in the Bacman reservoir. Alteration intensity is moderate to high and is often controlled by lithologic type and permeability. For example, andesite, volcanic breccia and sedimentary breccia units generally have moderate to high ~~intensity~~ alteration grade and moderate to abundant alteration intensity. However, microdiorites and hornfels from the deeper sections of well RS1D have weak alteration ~~intensity and few alteration minerals~~grade and intensity. Alteration minerals occur through replacement of primary minerals such as plagioclase and clinopyroxene, or through direct deposition in veins and vugs. Also, the alteration mineral assemblage indicates that the alteration grade increases with depth (i.e., prograding) for wells PAL18D, PAL30D, and RS1D, with temperature estimates increasing from 220 °C up to 280 °C. A common trend observed with increasing depth is increasing epidote crystallinity and concurrent appearance of index mineral geothermometers (from illite-smectite, to illite, to epidote, to wairakite/laumontite, to tremolite/actinolite). For well PAL8RD, the alteration grade stays uniform throughout the observed samples, yielding a temperature estimate of 240-260 °C. This estimate is in close agreement with the results of~~-~~ fluid inclusion homogenization temperatures (244°C) ~~analysis of~~from PAL8RD core samples ~~from~~ (Doma, ~~(~~2015). However, mineral paragenesis of the cuttings from the well shows relict alteration and multiple veining episodes, which indicates discordant conditions in the Kayabon reservoir. This reduces the current temperature estimate of the reservoir to 200-220 °C based on the presence of relict actinolite and sericite that retrograded to chlorite or sphene/leucoxene.

Whole rock major element chemistry ~~was employed~~ for PAL8RD samples serve as a supplement for the lack of comprehensive reservoir information~~ on this well~~. XRF results ~~data~~ show~~w there is~~ little variation with depth i~~o~~n silica and alkali concentrations (SiO_2 at 51.3~~0~~–53.8~~79~~%, K_2O at

1.14–2.15%, and Na_2O at 1.34–4.24%, see Supplemental Table 2). Meanwhile, there is an apparent increase in CaO ~~concentrations~~ wt% with depth from 7.81% at 1998 m to 16.27% at 2690 m, corresponding to changes in lithology.

4.2 Epidote chemistry

Generally, epidote ~~was observed as~~is subhedral to euhedral ~~crystals in~~with a prismatic or drusy habit, formed either in veins or as replacement of primary minerals such as plagioclase, clinopyroxene, and hornblende. It is often found associated with illite, chlorite, wairakite, and actinolite/tremolite. Chemically, there is an observable compositional variation in the epidote from~~s in~~ all four wells. The cation proportions computed from EMPA data can be approximated within the $Ca_2Fe_3Si_3O_{12}(OH)$–$Ca_2Al_3Si_3O_{12}(OH)$ binary system~~phase~~, with the mole fraction of $Ca_2Fe_3Si_3O_{12}(OH)$ (or X_{Fe}) generally ranging from 0.20 to 0.35.

Compositional variation in epidote demonstrates inversely proportional ~~is observed in inversely proportional fluctuations in measured~~ Al_2O_3 and FeO_t abundances, consistent with the common octahedral substitution between Fe^{3+} and Al^{3+} cations. Epidote Al_2O_3 varies from 19-29.4 wt. % (with a single outlier at 12.7 wt. %), while FeO_t varies from 6.3-18.2 wt. % (with the same outlier at 25.4 wt. % FeO_t). Stoichiometric~~ry~~ epidote mineral formulae, calculated on 12.5 oxygens per formula unit (pfu), contain 8 cations. However, epidote compositions reported here range primarily from 8.15 to 8.45 cations pfu, in close approximation to theoretical values. The "excess" observed cations are unlikely to be solely an analytical artifact, ~~the result of the analytical procedure~~ and instead also likely reflect real heterogeneity in the secondary epidote compositions. This is supported by inversely correlated Fe and Al abundances (both wt. % and calculated cations pfu) to total calculated cations. Despite this clear chemical correlation there is no observational relationship between the sum of Al^{3+} and Fe^{3+} cations and total calculated cations.

Chemical zonation within epidote~~s~~ is observed, particularly in the~~a~~ majority of epidote~~s~~ in PAL30D at 1700 m depth, wherein mineral cores ~~of the epidote~~ are more Al-rich than the rims, which are more Fe-rich. For example, a~~A~~t this depth, the Al_2O_3 content of a particular epidote grain in PAL30D (Fig. 2) is about ~~four percent richer~~4 wt% higher in the core than the rim (25.27% versus 21.50%, respectively), while the opposite is true for FeO_T content (11.31% at the core

versus 15.31% at the rim; Supplemental Table 1). This zonation is also evident in backscatter electron images with bright Fe-rich rims compared to darker Al-rich cores (Fig. 2).~~visually; wherein Al-rich cores register a darker shade of gray than Fe-rich rims in backscattered electron images of the mineral (Fig. 2).~~ Major element epidote compositions as a function of depth indicate a wide range in compositions at every depth interval (likely related to crystal zoning). Only PAL30D shows a weak systematic variation with depth, with average Al_2O_3 ± CaO concentrations decreasing with depth (with corresponding FeO_T~~Fe~~ increases; Fig. 3). Other wells have no evident systematic variations in epidote major element chemistry with depth of sampling.

4.3. Epidote isotopic composition

Results of isotopic analysis of hydrothermal epidote from ~~samples from~~ wells PAL18D, PAL30D, RS1D, and PAL8RD are presented in Table 1. The overall range of epidote δD ~~value of all epidotes collected in this study~~ is from -69.1‰ to -46.4‰, while for $\delta^{18}O$, the field-wide range is from 0.0‰ to ±11.6‰. Although sample numbers are limited, epidote average isotopic compositions are distinctly different between the four sampled wells. Average δD and standard deviation of analytical results per well ranges from -46.9 ± 0.6‰ (PAL8RD; n=5) to -64.2 ± 1.1‰ (RS1D; n=3). Inverse~~ly proportion~~ to the trend in δD, average $\delta^{18}O$ varies from 0.7 ± 0.6‰ (PAL8RD) to 10.5 ± 1.6‰ (RS1D), with average intermediate epidote isotope compositions for PAL18D (δD of -59.0 ± 9.2‰ and $\delta^{18}O$ of 6.2 ± 4.9‰; n=3) and PAL30D (δD of -56.2 ± 0.3‰ and $\delta^{18}O$ of 4.2 ± 0.3‰; n=3)~~ compositionally intermediate~~. In general, the δD and $\delta^{18}O$ values for PAL30D, RS1D, and PAL8RD epidote~~s~~ record relatively small ranges in isotopic composition~~, with commonly less than ~1.5‰ variance for either isotopic system~~. For these three wells, the δD range of epidotes only differs by 0.4‰, 2.1‰ and 1.6‰, respectively. Well PAL18D in contrast has a significant variation in both δD and $\delta^{18}O$ values, ranging from -69.1‰ to -51.1‰, and +0.5‰ to +9.8‰, respectively. Overall, there is no indication of a systematic change in epidote isotopic composition with depth of sampling (Table 1).

4.4. Fluid chemistry

For this study, liquid discharge data was~~ere~~ gathered from a total of 34 wells~~:~~; covering~~21 wells from~~ the Palayang Bayan sector (21), ~~five wells from~~the Botong sector (5), ~~four wells from~~ the

Cawayan sector (4), ~~three wells from~~the Tanawon sector (3), and ~~one well from~~the Rangas sector (1). This~~ese~~ includes physical and chemical parameters such as composition, discharge enthalpy, sampling pressure, and pH. Full results are available in the online supplement. Results indicate that all geothermal well discharges are alkali-chloride fluids ~~having~~ with a near~~-~~-neutral pH.

~~Chloride is dominant among the components measured in the geothermal well discharge samples.~~ As a conservative component in the fluid, ~~along with boron (B),~~ Cl (and B) tend~~s~~ to stay ~~dissolved~~ within the liquid phase (Arnórsson and IAEA, 2000). Among the wells, chloride concentrations are high, with reservoir values ranging from 1,822 to 12,344 mg/kg. Boron ~~has a much~~concentrations are significantly lower ~~concentration~~ in the fluids, with measured values varying from 13.6 to 353 mg/kg. Across the geothermal field, the average molar ratio of Cl/B ~~calculated from measured abundances~~ is 57. Homogeneity in molar Cl/B is better reflected in the different sectors. Wells in Tanawon and Cawayan sectors have relatively high Cl/B values (average of 71 and 65, respectively), while wells in Palayang Bayan sector have moderate Cl/B values (ranging widely from 33 to 79, with an average of 63). These wells are in stark contrast to wells in Botong and Rangas sectors, which have low to very low molar ratios (23 and 6, respectively; Fig. 4b).

Reservoir δD (δD_{res}) values for Bacman well discharges range from ~~around~~ approximately -23.5‰ (well RS1D, Rangas sector) to -17.9‰ (PAL23D, Palayang Bayan sector) ~~relative to V-SMOW~~ and have an average of -20.0‰. For reservoir $\delta^{18}O$ ($\delta^{18}O_{res}$), ~~values for the~~ fluid samples range from -3.32‰ (CN1, Cawayan sector) to +7.2‰ (RS1D) ~~relative to V-SMOW~~. The average $\delta^{18}O_{res}$ for the Bacman reservoir is -0.90‰. Overall, wells in the Botong and Rangas sectors have the most depleted ~~fluids based on~~ δD_{res} and the most enriched ~~fluids based on~~ $\delta^{18}O_{res}$, with fluid from RS1D representing the lowest δD_{res} and highest $\delta^{18}O_{res}$ in the Bacman reservoir. Increasing δD_{res} and decreasing $\delta^{18}O_{res}$ occurs westward towards the Palayang Bayan, Tanawon, and Cawayan sectors (Fig. 5b). For wells with corresponding epidote isotopic analyses, PAL18D and PAL30D, δD_{res} is -23.0‰ and -21.0‰ while $\delta^{18}O_{res}$ is -0.6‰ and -2.4‰, respectively (Table 1; PAL18D from Ruaya et al., 1993). No fluid isotopic data is available for well PAL8RD. ~~These isotopic~~Isotopic and chemical differences between sectors ~~in the field~~ are attributed to the influence of peripheral fluids (Solis et al., 1998) and ~~effect of~~ fluid extraction ~~in~~ from the reservoir (see section 5.2; Espartinez and See, 2015) ~~and is thoroughly discussed in section 5.2~~.

5. Discussion

5.1. Epidote-fluid disequilibrium

Host rock compositions and lithology appear to exert significant influence on the major element composition of epidote~~s~~ (See Table 2 and Supplemental Table 2), likely through replacement of primary minerals during progressive fluid-~~-~~rock interaction. For well PAL8RD, there is a correlation between the ~~composition between whole rock XRF data~~whole rock and epidote compositions ~~and epidote microprobe data~~ (Fig. 6). Results suggest that the $Ca_2Fe_3Si_3O_{12}(OH)$ mole fraction of epidote~~s~~ correlates well with the Fe/(Fe+Al) oxide ratio of the cuttings. Likewise, variations in the trace element oxides in epidote such as MgO and Na_2O ~~are~~ correlate~~d~~ with whole rock composition, particularly on the three deepest samples from the well at 2298, 2388 and 2690 m (Fig. 6).

In addition to reservoir lithology, fluid chemistry ~~can have a significant role in~~may also affect the major-element composition of epidote (Giggenbach, 1984; Arnason and Bird, 1992; Arnason et al., 1993). ~~For~~ In the case of epidote Fe-Al chemical zonation ~~observed in some epidotes in all four wells~~, fluid~~s~~ parameters such as temperature, pH, and O_2 and CO_2 fugacity may significantly influence epidote Fe^{3+} and Al^{3+} molar proportions (Fe^{3+}/Al^{3+}; Arnason et al., 1993). Distinguishing between these factors in a dynamic system is challenging and beyond the scope of this investigation. For example, assuming constant fluid compositions, the increasing X_{Fe} can result from decreasing formation temperatures. ~~However, in near-pH neutral fluids at the 250-300°C temperatures based on downhole measurements in Bacman wells~~Further, the solubilities of $Fe(OH)_3$ and $Al(OH)_4^-$, the primary Fe^{3+} and Al^{3+} complexes at ~~these conditions~~near-neutral pH and elevated temperatures (>200°C), are also dependent on fluid pH (Arnason et al., 1993). ~~Under conditions of the Bacman wells~~At conditions of the Bacman wells (242-301°C, see Table 1), the increase of ~0.1 X_{Fe} in epidote rims can result from a relatively small increase (~0.25-0.3) in pH, at constant temperatures (Arnason et al., 1993). ~~From these results,~~ W~~w~~e conclude that ~~that epidote here records mineral-rock-fluid disequilibrium whereby~~ the average or "bulk" major-element composition of epidote is ~~dictated~~ strongly influenced by ~~the~~ host-rock mineralogy and chemistry, while ~~mineral~~ epidote zonation instead likely reflects subtle changes in fluid chemistry.

Mineral and fluid chemistry ~~data from this study show~~demonstrate that the composition of epidote~~s~~ in the Bacman field is largely dependent on fluid mixing and water-rock interaction. The isotopic composition of the fluids (Fig. 7;~~.~~ See also Supplemental Table 4 for the complete fluid isotopic data~~.~~) indicate that the Bacman geothermal field, as an andesitic geothermal system along a convergent plate boundary, typifies the "classical" $\delta^{18}O$ isotope enrichment of fluids relative to meteoric waters (Bacman $\delta^{18}O$ = -4.8‰; Salonga, 2015). This enrichment is often due to water-rock interaction and mixing with fluids having isotopic compositions close to magmatic end members (~~(~~Craig, 1963; Giggenbach, 1992). For example, at the extreme compositional end, we see that well RS1D fluid ($\delta^{18}O$ at +7.2‰ and δ D at -23.5‰) coincides with fumarolic condensates from andesitic volcanoes in the Philippines and is similar to andesitic or "magmatic" fluids as defined by Giggenbach (1992). Further, this study demonstrates the dependence of rock and mineral isotopic composition ~~not only~~ on reaction processes and coupled varying fluid-rock ratios (Bowers and Taylor, 1985; Lee and Bethke, 1996; Kleine et al., 2018), ~~but also on~~as well as on temperature-dependent equilibrium fractionation constants~~, which are ultimately dependent on temperature~~ (Chacko et al., 1999). Thus, what controls the O- and H-~~-~~isotope composition of ~~the~~ epidote~~s~~ is the degree of fluid-rock buffering and the temperature ~~that~~ of epidote growth ~~occurs at~~.

From the calculated equilibrium fluids ($\delta_{fluid(eq)}$; Equations 10 and 11), variations in both δD ~~hydrogen~~ and $\delta^{18}O$ ~~oxygen isotopes~~ are evident when compared to measured δ_{fluid} ~~(Table 1)~~. The discharge fluid samples represent a modern, "final" or average fluid composition and do not necessarily represent the heterogeneity of fluids at depth as recorded by epidote, or potential changes in the composition of fluids over time (Table 1). Intra-well variations thus reflect the effectivity of epidote in recording vertical isotopic variations of the fluids in equilibrium with the mineral. Currently, the fluids discharging from wells are isotopically distinct (δD = -23.5‰ to -17.9‰; $\delta^{18}O$ = -3.32‰ to +7.2‰; Supplemental Table 4) from the calculated epidote-equilibrium fluids ~~from which epidotes formed~~($\delta D_{fluid(eq)}$ = -38.6‰ to -19.3‰; $\delta^{18}O_{fluid(eq)}$ = -2.4‰ to +10.3‰; Table 1). ~~in equilibrium with.~~

By comparing the fractionation factors between the epidote and well discharges to isotopic equilibrium for D/H (Chacko et al., 1999) and $^{18}O/^{16}O$ (Pope et al., 2016) as a function of temperature, we can assess the current relative epidote-fluid disequilibrium in isotopic space (Fig. 8). Fractionation factors are skewed away from the theoretical isotopic equilibrium based on

modern downhole well temperatures, to a lesser extent for D/H and more significantly for $^{18}O/^{16}O$. In addition, several calculated fractionation factors are out of thermal equilibrium, defined by the temperature range where the occurrence of hydrothermal epidote~~s~~ is expected in Bacman or in other geothermal fields (180-320°C; Reyes, 1985; Reyes, 1990; Bird and Spieler, 2004). However, based on uncertainty in D/H fractionation by Chacko et al. (1999) considered to be ±10‰, most data points could still be included within the theoretical range of hydrogen isotope equilibrium. Given that proportionally hydrogen is far less abundant in rocks compared to the fluid, the disequilibrium of fluid D/H may readily reflect changes in fluid isotopic composition. Meanwhile, the $^{18}O/^{16}O$ fractionation factors are skewed ~~away~~ to a greater degree from ~~the~~ isotopic equilibrium, which suggest a greater fluid-epidote disequilibrium than observed in D/H space (Fig. 8). This~~,~~ likely ~~reflecting~~ reflects the significant oxygen buffering by the host rock. In short, similar to the complex nature of major elements discussed above, D/H ~~isotopes~~ reflects potential changes in fluid compositions while $^{18}O/^{16}O$ likely instead reflects the complexity of variable fluid-rock interactions.

5.2. Changes in Fluid Composition

Stable isotope ~~data~~ compositions of~~from~~ geothermal fluids were gathered ~~as part of the baseline hydrothermal fluid data~~ to define the baseline chemistry (Ruaya et al., 1993) and hydrogeology (Caranto, 1999) of the Bacman geothermal field, ~~and also~~necessary for monitoring reservoir changes during field operations (Martinez-Olivar et al., 2005). Ruaya et al. (1993) ~~illustrated~~ determined that the composition of discharge fluids from Bacman geothermal wells are heavily affected by water-rock interaction, ~~where fluids are said to be isotopically shifted with respect to~~with shifts in the fluid oxygen isotopes from the global meteoric water line (Giggenbach, 1992). The spatial variation of $\delta^{18}O_{res}$~~,~~ ~~also resembles~~similar to the Cl_{res} and T_{quartz} ~~trends and shows~~variations, demonstrates that wells with higher $\delta^{18}O_{res}$ values (~+3.00‰) are located close to Botong sector (Fig. 5a). These isotopic values gradually decrease for wells in the Palayang Bayan and Cawayan sectors, which get closer to the fringes of the reservoir and are more likely to have significant meteoric water input (Martinez-Olivar et al., 2005).

Changes in the chemical characteristics of fluids in the Bacman geothermal field are evident since the start of commercial operation (Fig. 4, 5; Espartinez and See, 2015; Ramos and Espartinez,

2015). On average, wells in the Botong sector still have the most isotopically enriched fluids among the rest of the field, when oxygen isotope data from this study are compared with baseline values from Ruaya et al. (1993), although the single Rangas well ~~has~~ maintains the most enriched $\delta^{18}O_{res}$ fluid (Fig. 5). Although the same spatial trends in $\delta^{18}O_{res}$ exist with increasing isotopic depletion to the west, ~~the movement of~~shifting -2‰ and -1‰ contour lines (Fig. 5) to the east from the Cawayan sector to the Palayang Bayan sector is observed when compared to the ~~original contour figure from the~~ baseline data of Ruaya et al. (1993). This suggests that the onset of production ~~stage~~ in the Bacman field has also ushered the movement of isotopically depleted fluids from the west of the field to the main portion of the reservoir.

The molar ratio of chloride and boron (Cl/B) from well discharge fluids compared to initial conditions indicates a similar trend as observed in $\delta^{18}O_{res}$ data (Fig. 4; Ruaya et al., 1993). Comparison of ~~the~~ molar Cl/B contours (Fig. 4) shows the movement of peripheral fluids from the west towards the central Bacman reservoir. There is a noticeable increase in Cl/B ~~values~~ based on fluid samples from this study, where fluids with high Cl/B values (~60 to 75) have now moved to the southern Palayang Bayan sector and east of the Cawayan and Tanawon sectors. This clearly ~~represents~~ demonstrates that the geothermal field is already tapping a different type of fluid coming from the western periphery of the reservoir. This trend was first observed shortly after the onset of production, and it was suggested that continuous fluid extraction from the wells prompted fluids that come from the Masakrot area in the immediate western periphery of the field to migrate eastwards (Solis et al., 1998). These geothermal fluids are characterized as relatively cooler, and isotopically depleted ~~and degassed fluids~~ compared to those coming directly from the reservoir. The migration of Masakrot fluids is also regarded as the reason for ~~the~~ only a minimal decline in reservoir pressure in the field (Solis et al., 1998). On the other hand, the increase in Cl_{res}, especially for most wells in the Palayang Bayan sector can be explained by ~~fluids from geothermal wells injected~~reinjection of well fluid back into the reservoir (Fig. 9). Geothermal fluids extracted from production wells and separated from steam are relatively cooler and have low gas content, but have high solute concentrations when ~~injected back~~reinjected. In Bacman, injection sinks are located away from the main production area, towards the northwest in the Palayang Bayan sector and further west in the Cawayan sector. However, due to continuous extraction and injection of fluids, the incursion of injection fluids ~~have~~ has already manifested in the form of a steady increase in

Cl_{res}, to concentrations ~~which~~that approach ~~that of~~the injection fluids, particularly in the northern part of the Palayang Bayan sector and in the Cawayan sector (Espartinez and See, 2015).

In contrast to regional trends, there is a noticeable enrichment in $\delta^{18}O_{res}$ values of fluids from wells OP3D (Δ +0.69‰) and OP4D (Δ +0.55‰) in the Botong sector (Fig. 9). This enrichment suggests that localized boiling is expanding within the reservoir ~~at~~ in the Botong sector due to fluid extraction, and that these wells are tapping residual fluids. Although b~~B~~oiling in the reservoir ~~has been~~is occurring ~~in the natural state~~, ~~but~~ it is currently limited ~~only~~ to the Botong sector (Ruaya et al., 1993; Martinez-Olivar et al., 2005). Data from Martinez-Olivar et al. (2005) showed that the $\delta^{18}O_{res}$ of OP6D had been depleted to +0.72‰, which suggests that OP6D has already been tapping steam condensates (Fig. 9). Meanwhile for wells tapping the residual fluids, it is expected that they would have manifested an isotopic enrichment and/or increase in solute concentrations, such as the case of wells OP3D and OP4D (Fig. 9; Supplemental Table 3). As boiling near the reservoir upflow continues, it ~~can be~~is expected that the vapor-rich zone forming in the reservoir could expand not just in Botong sector, but also ~~well~~ into the Palayang Bayan sector and the rest of the field.

5.3. Hydrogeological model of Bacman

By integrating various geochemical data from well discharge fluids and reservoir rocks, this study shows that the influence of particular reservoir processes on the evolution of fluids differs ~~from one location to another~~between locations in the reservoir. Here we present an updated and expanded Bacman hydrogeological model that summarizes the effect of fluid mixing and water-rock interaction on the present configuration of the Bacman reservoir in the Palayang Bayan and Botong sectors. Also, we have now incorporated in this model the reservoir processes occurring in the exploration sectors of Rangas and Kayabon (Fig. 10).

The present and widely-accepted hydrogeological model ~~by most authors~~for the Bacman reservoir (e.g., Reyes, 1985; Zaide-Delfin et al., 1989; Ruaya et al., 1993; D'Amore et al., 1993; and Ramos and Santos, 2012) points to Botong sector, specifically underneath Mt. Pangas, as the location of the main heat source and upflow region. ~~for the Bacman reservoir.~~ This model has been contested in the past (e.g., Reyes et al., 1995) due to the existence of other volcanic centers in Bacman that

were postulated to be separate heat sources. However, beyond this ~~assumption~~inference, there ~~have~~ has been no conclusive data that could constrain these areas ~~until the~~prior to drilling wells RS1D and PAL8RD ~~were drilled~~.

Petrologic and geochemical data of well RS1D in the Rangas sector presented a strong case ~~that~~ for a heat source distinct from the one in the Botong sector ~~does exist in Rangas~~ (Santos, 2014; Ramos et al., 2015). However, subsequent drilling in the Rangas sector showed subpar temperature estimates and limited wellbore permeability relative to RS1D and other wells in the Bacman field (Ramos et al., 2015)~~, which suggested that Rangas has a separate but localized heat source~~. Here, we agree with previous studies (Ramos, 2002; Santos, 2014; Ramos et al., 2015) that the source of fluids in RS1D is ~~also coming from~~the Botong sector, where a small component of hydrothermal fluids flows southeast towards the Rangas sector along permeable faults. The fluid~~s~~ and epidote~~s~~ in the Rangas sector are isotopically more enriched (~~based on~~ $\delta^{18}O$) compared to any other wells in the field. We argue that the most-likely mechanism for $\delta^{18}O$ isotopic enrichment of fluids in the Rangas sector is through a higher degree of water-rock interaction ~~with reservoir rocks~~. This is similar to what was presented by Ruaya et al. (1993) to explain the enriched $\delta^{18}O$ compositions of fluids from Botong wells through intensive interaction with carbonates in the reservoir. This too may have ~~likely happened~~occurred when fluids from the upflow region travelled laterally through faults and fractures to the Rangas sector, resulting in~~to~~ greater fluid isotopic enrichment. High B ~~concentration~~ in the fluid (and low Cl/B) from the Rangas sector well may further corroborate this model, with the high B reflecting extensive interaction with reservoir rocks (Arnórsson and IAEA, 2000).

For the Palayan Bayan sector, wells PAL18D and PAL30D present contrasting chemical and isotopic compositions of epidote and equilibrium calculated fluids. ~~based on the epidotes and the calculated fluids in equilibrium with the minerals.~~ The heterogeneous isotopic composition~~s~~ of PAL18D epidote~~s~~ is~~are~~ in stark contrast with the relatively consistent compositions of PAL30D epidote~~s~~, suggesting that the two wells have experienced different reservoir conditions in the Palayang Bayan sector as a result of differential fluid mixing and water-rock interactions. PAL18D fluids may ~~have resulted through~~be the result of mixing of meteoric (Bacman $\delta^{18}O$ = -4.8‰; Salonga, 2015) and magmatic waters (e.g. δD -20 to -29‰ and $\delta^{18}O$ +2.6 to +8‰ as defined by fumerole condensates from Philippine arc volcanoes; Giggenbach, 1992) in varying degrees

throughout the evolution of the geothermal reservoir. Meanwhile, the PAL30D fluid likely evolved through continuous fluid mixing in the past. The onset of fluid extraction in the Bacman field has accelerated this fluid evolution, ~~making the PAL30D fluid~~with more enriched ~~in~~ δD_{res} and more depleted ~~in~~ $\delta^{18}O_{res}$ in the PAL30D fluid.~~.~~

Compared with hydrothermal epidote~~s~~ elsewhere in the Bacman system, the epidotes from well PAL8RD in the Kayabon sector retain isotopic signatures in equilibrium with distinct fluid compositions (based on D/H and arguments above about controls on epidote isotopic compositions). The petrogenesis of Kayabon epidote~~s~~ is ~~deemed~~ interpreted ~~an earlier event~~to have formed from a ~~previously hotter heat~~higher temperature source, prior or contemporaneous to when fluids in the main part of the reservoir were still more isotopically enriched than their present compositions (Ruaya et al., 1993; Martinez-Olivar et al., 2005). Also, the calculated epidote-equilibrium fluid ~~with epidote~~ is similar to the isotopic~~e~~ compositions of PAL18D and PAL30D discharge fluids. The depleted nature of calculated PAL8RD fluid, relative to PAL18D, PAL30D, and RS1D fluids, suggests a distinct source ~~from~~ relative to the fluids originating from the Palayang Bayan or Rangas sectors. However, ~~with respect to hydrogen isotopes,~~ the enriched H-isotopic nature of the~~is~~ fluid and ~~the~~ epidote~~s~~ in PAL8RD, relative to ~~the respective fluid and epidote samples of the~~those in other wells in this study ~~come into question since it~~ is unusual, since ~~for~~ fluids in equilibrium with the reservoir rocks tend to have elevated δD. One possible explanation is ~~the~~ that ~~presence of~~ pre-existing hydrous silicates ~~that were involved in~~influenced water-rock reactions~~interaction~~ in the Kayabon sector, producing enriched D/H epidote. ~~to produce the epidotes that were sampled.~~ Interaction of meteoric water and relatively fresh rock may have commenced ~~earlier in the hotter ancient~~prior to modern geothermal activity in the ~~-~~Kayabon reservoir, producing these preexisting hydrous silicates.~~and may have produced these preexisting hydrous silicates, which resulted to increased D/H values of Kayabon epidotes from the onset compared to the rest of the Bacman reservoir.~~ Subsequent interactions of the altered rock with meteoric water ~~fluids~~ in modern reservoir conditions ~~close to the present~~ may have resulted in further ~~increase~~ enrichment in D/H to present-day compositions. A similar interpretation exists for the Hakone geothermal system where substantial groundwater recharge fluids led to the long-term δD enrichment and δ18O depletion of both fluids and host rock~~values until they reached present compositions. This is similar to the characteristics of fluids in Hakone geothermal system~~ (Matsuo

et al., 1985; Giggenbach, 1992)~~, where substantial involvement of recharge fluids from the groundwater enriched the δD values in both the rocks and fluids, and depleted them with in $\delta^{18}O$ at the same time.~~.

6. Conclusions

Investigating the chemical and isotopic properties of well discharge fluids and hydrothermal epidote~~s~~ reveals the spatial variation and temporal evolution ~~undergone by~~of the hydrothermal fluids and reservoir rocks across the Bacon-Manito Geothermal Field. These changes ~~through space and time have been~~are the result of a combination of fluid mixing and water-rock interaction, which have largely influenced the present configuration of the geothermal reservoir. The $\delta D_{epidote}$ ~~values~~ w~~ere~~as found to be generally in equilibrium with present-day geothermal fluids~~ from well discharges~~. ~~On the contrary~~In contrast, $\delta^{18}O_{epidote}$ ~~values were~~was not in mineral-fluid equilibrium, suggesting a greater sensitivity to reservoir processes for~~that~~ epidote oxygen isotopes~~ are more sensitive to prevailing reservoir processes compared to hydrogen isotopes~~. As~~,~~ such, the~~at~~ variations in $\delta^{18}O_{epidote}$ ~~values~~ better reflects the effects of boiling, fluid mixing and/or water-rock interaction ~~better than~~compared to $\delta D_{epidote}$~~ values~~.

Comparison of baseline fluid chemistry to present-day concentrations with ~~datasets from the reservoir's natural state and the present state during~~ continuous field operations, particularly increasing molar Cl/B and decreasing $\delta^{18}O$ across the field, has ~~clarified the occurrence of~~revealed several reservoir processes, such as localized boiling in the Botong sector and incursion of peripheral waters and injection fluids in the Palayang Bayan and Cawayan sectors. ~~This was indicated by significant changes in calculated geochemical parameters such as increase in molar Cl/B ratio and decrease in $\delta^{18}O$ across the field relative to baseline values.~~ Meanwhile, epidote chemistry reflects variations in whole rock composition, fluid composition and the degree of ~~, and, related to both, the amount of~~ fluid~~water~~-rock interaction. Major-element c~~C~~hemical zoning in epidote is likely related to variations in fluid chemistry (e.g. temperature, pH) whereas average epidote composition~~s~~ reflects host ~~lithologies~~compositions. ~~Similarly, epidote~~Epidote D/H variations are largely near-equilibrium with fluids, based on fractionation factors and downhole temperatures, while epidote $^{18}O/^{16}O$ compositions reflect variable water-rock interaction.

The combined results from this study and literature data enable us to formulate an updated and more comprehensive hydrogeological model of the Bacman reservoir. We present here that the main heat source of the field is located beneath Mt. Pangas in the Botong sector and that the fluids originating in the upflow of the resource vary spatially and evolve temporally due to a combination of reservoir processes. ~~And~~ L~~l~~astly, while evidence indicate ~~that~~ the existence of heat sources in the Rangas and Kayabon ~~exist~~sectors, these heat sources appear to be localized for the Rangas sector and ~~appear to~~ have waned through time in the Kayabon sector.

7. **Conflict of Interest Statement**

First author Julius Dimabayao was funded to conduct research presented in this manuscript as part of his MSc at the University of Auckland on the Bacon-Manito Geothermal Field (Bacman) by Energy Development Corporation (EDC) and is an employee of the EDC. Interpretations were developed independent of EDC input as independent research at the University of Auckland.

8. Acknowledgement

This study was made possible through the support of the Energy Development Corporation and the Bacman Geothermal Business Unit, for providing the drill cuttings and data for the fluid discharge samples, and for funding the isotopic analysis. We also thank the School of Environment, University of Auckland for providing the funding for whole rock and microprobe analysis. Special thanks are given to Josephine Rosell, Andres Arcila Rivera, Ilyas Qasim, and Ian Schipper for their assistance in the various analyses performed in this study. We would also like to thank two anonymous reviewers for their detailed and helpful comments to improve this manuscript.

References

Abrigo, F., Bayon, F. E., See, F., Siega, F., Sunio, E., 2006. General Trends and Characteristics of Philippine Geothermal Gases. A Joint Scientific Study of PNOC-EDC and Unocal Philippines. Makati City, Philippines.

Andal, E. S., Yumul, G. P., Listanco, E. L., Tamayo, R. A., Dimalanta, C. B., Ishii, T., 2005. Characterization of the Pleistocene volcanic chain of the Bicol Arc, Philippines: Implications for geohazard assessment. Terrestrial Atmospheric and Oceanic Sciences, 16(4), 865-883.

Arnason, J. G., Bird, D. K., 1992. Formation of zoned epidote in hydrothermal systems. Proceedings 7th International Symposium on Water-Rock Interactions. Park City, Utah, pp. 1473-1476.

Arnason, J. G., Bird, D. K., Liou, J. G., 1993. Variables controlling epidote composition in hydrothermal and low-pressure regional metamorphic rocks. Proceedings 125 Years Knappenwand. Salzburg, Austria, pp. 17-25.

Arnórsson, S., International Atomic Energy Agency, 2000. Isotopic and chemical techniques in geothermal exploration, development and use. International Atomic Energy Agency. Vienna, Austria.

Bertani, R., 2015. Geothermal Power Generation in the World 2010-2014 Update Report. Proceedings World Geothermal Congress 2015. Melbourne, Australia.

Bird, D. K., Cho, M., Janik, C. J., Liou, J. G., Caruso, L. J., 1988. Compositional, Order/Disorder, and Stable Isotope Characteristics of Al- Fe Epidote, State 2–14 Drill Hole, Salton Sea Geothermal System. Journal of Geophysical Research: Solid Earth, 93(B11), 13135-13144.

Bird, D. K., Spieler, A. R., 2004. Epidote in geothermal systems. Reviews in Mineralogy and Geochemistry, 56(1), 235-300.

Bowers, T. S., Taylor, H. P., 1985. An integrated chemical and stable-isotope model of the origin of midocean ridge hot spring systems. Journal of Geophysical Research: Solid Earth, 90(B14), 12583-12606.

Bruinsma, J. W., 1983. Results of potassium-argon age dating on twenty rock samples from the Pinatubo, Southeast Tongonan, Bacon-Manito, Southern Negros and Tongonan, Leyte areas, Philippines. Proprietary Report by Robertson Research Ltd. to PNOC-EDC, 24 p.

Caranto, J. A., 1999. Integrated Hydrogeological Study of Bacon-Manito Geothermal Production Field and Surrounding Areas. Technical Report, PNOC-EDC.

Cartwright, I., Buick, I. S., Vry, J. K., 1996. Polyphase metamorphic fluid flow in the Lower Calcsilicate Unit, Reynolds Range, central Australia. Precambrian Research, 77(3), 211-229.

Chacko, T., Riciputi, R., Cole, R., Horita, J., 1999. A new technique for determining equilibrium hydrogen isotope fractionation factors using the ion microprobe: Application to the epidote-water system. Geochimica et Cosmochimica Acta, 63(1), 1-10. doi:10.1016/S0016-7037(99)00007-1

Craig, H., 1961. Standard for reporting concentrations of deuterium and oxygen-18 in natural waters. Science, 133, 1833–1834.

Craig, H., 1963. The isotopic geochemistry of water and carbon in geothermal areas. Proceedings Conference on Nuclear Geology on Geothermal Areas. Pisa, Italy, pp. 17-53.

D'Amore, F., Maniquis-Buenviaje, M., Solis, R., 1993. An Evaluation of the Deep Reservoir Conditions of the Bacon-Manito Geothermal Field, Philippines using Gas Chemsitry. Proceedings 18th Workshop on Geothermal Reservoir Engineering. Stanford, California, pp. 235-240.

Department of Environment and Natural Resources–Mines and Geosciences Bureau (DENR-MGB), 2004. In Aurelio, M. A., Peña, R. E. (Eds.), Geology and mineral resources of the Philippines (Revised edition). DENR-MGB, Quezon City, Philippines.

Doma, L. D., 2015. Petrology of Well PAL8RD (KB1D). Technical Report, EDC.

Espartinez, C. M. R., See, F. S., 2015. The BacMan Geothermal Field, Philippines: Geochemical changes and challenges after twenty years of operation. Proceedings World Geothermal Congress 2015. Melbourne, Australia.

Fournier R.O., 1977. Chemical geothermometers and mixing models for geothermal systems. Geothermics, 5, 41-50.

Fournier, R. O., Truesdell, A. H., 1974. Geochemical indicators of subsurface temperature--2. Estimation of temperature and fraction of hot water mixed with cold water. U.S. Geol. Survey J. Res. 2, 263-270.

Frei, D., Liebscher, A., Franz, G., Dulski, P., 2004. Trace element geochemistry of epidote minerals. Reviews in Mineralogy and Geochemistry, 56(1), 553-605.

Giggenbach, W. F., 1984. Mass transfer in hydrothermal alteration systems—a conceptual approach. Geochimica et Cosmochimica Acta, 48(12), 2693-2711.

Giggenbach, W. F., 1992. Isotopic shifts in waters from geothermal and volcanic systems along convergent plate boundaries and their origin. Earth and Planetary Science Letters, 113(4), 495-510.

Graham, C. M., Sheppard, S. M. F., 1980. Experimental hydrogen isotope studies, II: fractionations in the systems epidote-NaCl-H_2O, epidote-$CaCl_2$-H_2O and epidote-seawater, and the hydrogen isotope composition of natural epidotes. Earth and Planetary Science Letters, 49, 237-251.

Graham, C. M., Sheppard, S. M. F., Heaton, T. H. E., 1980. Experimental hydrogen isotope studies –I. Systematics of hydrogen isotope fractionation in the systems epidote-H_2O, zoisite-H_2O and AlO(OH)-H_2O. Geochimica et Cosmochimica Acta, 44, 353-364.

Horita, J., Wesolowski, D. J., 1994. Liquid-vapor fractionation of oxygen and hydrogen isotopes of water from the freezing to the critical temperature. Geochimica et Cosmochimica Acta, 58(16), 3425-3437.

Japan International Cooperation Agency (JICA), 1999. Report on regional survey for mineral resources in the Bicol area, the Republic of the Philippines: Final Report. Japan.

Keith, T., Muffler, L., Cremer, M., 1968. Hydrothermal epidote formed in Salton Sea Geothermal System, California. American Mineralogist, 53(9-10), 1635-1644.

Kleine, B.I., Stefansson, A., Halldorsson, S.A., Whitehouse, M.J., Jonasson, K., 2018. Silicon and oxygen isotopes unravel quartz formation processes in the Icelandic crust. Geochemical Perspectives Letters, 7, 5-11.

Kohn, M. J., Valley, J. W., 1998. Oxygen isotope geochemistry of the amphiboles: Isotope effects of cation substitutions in minerals. Geochimica et Cosmochimica Acta, 62, 1947-1958.

Lawless, J., Bromley, C., Leach, T., Licup, A., Cope, D., Recio, C., 1983. Bacon-Manito Geothermal Field: A geoscientific exploration model. Proceedings 5th New Zealand Geothermal Workshop, pp. 97-102.

Lee, M. K., & Bethke, C. M., 1996. A model of isotope fractionation in reacting geochemical systems. American Journal of Science, 296(9).

Martinez-Olivar, M. V. M., See, F., Solis, R., 2005. Isotopic Response to Changes in the Reservoir in Bacman Geothermal Production Field, Philippines. Proceedings World Geothermal Congress 2005. Antalya, Turkey.

Matsuhisa, Y., Goldsmith J. R., Clayton R. N., 1979. Oxygen isotopic fractionation in the system quartz-albite-anorthite-water. Geochimica et Cosmochimica Acta, 43, 1131-1140.

Matsuo, S., Kusakabe, M., Niwano, M., Hirano, T., Oki, Y., 1985. Origin of thermal waters from the Hakone geothermal system, Japan. Geochemical Journal, 19(1), 27-44.

Matthews, A., Goldsmith, J. R., Clayton, R. N., 1983. Oxygen isotope fractionation between zoisite and water. Geochimica et Cosmochima Acta, 47, 645-654.

Moeck, I., 2014. Catalog of geothermal play types based on geologic controls. Renewable and Sustainable Energy Reviews, 37, 867-882. doi:10.1016/j.rser.2014.05.032

Morrison, J., 2004. Stable and radiogenic isotope systematics in epidote group minerals. Reviews in Mineralogy and Geochemistry, 56(1), 607-628.

O'Neil, J.R., 1986. Theoretical and experimental aspects of isotopic fractionation. Reviews in Mineralogy and Geochemistry, 16, 1-40.

Ozawa, A., Tagami, T., Listanco, E. L., Arpa, C. B., Sudo, M., 2004. Initiation and propagation of subduction along the Philippine Trench: evidence from the temporal and spatial distribution of volcanoes. Journal of Asian Earth Sciences, 23(1), 105-111.

Panem, C. C., Alincastre, R. S., 1985. Surface geology of the Bacon-Manito Geothermal Reservation. Technical Report, PNOC-EDC

Patrier, P., Beaufort, D., Touchard, G., & Fouillac, A. M., 1990. Crystal size of epidotes: a potentially exploitable geothermometer in geothermal fields? Geology, 18(11), 1126-1129.

Pope, E. C., Bird, D. K., Arnórsson, S., 2014. Stable isotopes of hydrothermal minerals as tracers for geothermal fluids in Iceland. Geothermics, 49, 99-110.

Pope, E. C., Bird, D. K., Arnórsson, S., Giroud, N., 2016. Hydrogeology of the Krafla geothermal system, northeast Iceland. Geofluids, 16, 175-197. doi: 10.1111/gfl.12142

Ramos, S. G., 2002. Potential Constraints to the Development of the Rangas Sector based on Petrologic Evaluation of the Bacman Geothermal Field, Philippines. Proceedings 27th Workshop on Geothermal Reservoir Engineering. Stanford, California.

Ramos, M. E. S., Espartinez, C. M. R., 2015. The Bacon-Manito surface thermal features–geochemical and physical changes after three decades (1983-2013) of Monitoring. Proceedings World Geothermal Congress 2015. Melbourne, Australia.

Ramos, S. G., Santos, B. N. E. A., 2012. Updated Hydrogeological Model of the Bacon-Manito Geothermal Field, Philippines. Proceedings 37th Workshop on Geothermal Reservoir Engineering. Stanford, California.

Ramos, S. G., Padrique, M. G. C., Jara, M. P., 2015. Conceptual Hydrogeological Model of the Rangas Sector, Bacman Geothermal Field, Philippines. Proceedings World Geothermal Congress 2015. Melbourne, Australia.

Reyes, A. G., 1985. A comparative study of "acid" and "neutral pH" hydrothermal alteration in the Bacon-Manito Geothermal Area, Philippines. Master of Science in Geology Thesis, University of Auckland. Auckland, New Zealand.

Reyes, A. G., 1990. Petrology of Philippine geothermal systems and the application of alteration mineralogy to their assessment. Journal of Volcanology and Geothermal Research, 43(1), 279-309. doi:10.1016/0377-0273(90)90057-M

Reyes, A. G., Zaide-Delfin, M. C., Bueza, E. L., 1995. Petrological Identification of Multiple Heat Sources in the Bacon-Manito Geothermal System, Philippines. Proceedings World Geothermal Congress 1995. Florence, Italy, pp. 713-717.

Ruaya, J. R., Buenviaje, M. M., Solis, R. P., Gonfiantini, R., 1993. Chemical and Isotopic Studies in the Bacon-Manito Geothermal Field, Philippines. Proceedings Application of Isotope and Geochemical Techniques to Geothermal Exploration in the Middle East, Asia, the Pacific and Africa. Dumaguete City, Philippines, pp. 185-208.

Salonga, N. D., 2015. Estimating the Isotopic Composition of Meteoric Water Index in Geothermal Fields in the Philippines. Proceedings 2015 World Geothermal Congress 2015, Melbourne, Australia.

Santos, B. N. E. A., 2014. Thermometric Indicators of Fluid-Rock Interaction in the Bacon-Manito Geothermal Field, Philippines. Master of Science in Geology Thesis, University of Auckland. Auckland, New Zealand.

Scientech, LLC (2005). PEPSE Steam Tables [Computer software]. Idaho falls, ID.

Sharp, Z. D., 1990. Laser-based microanalytical method for the in situ determination of oxygen isotope ratios of silicates and oxides. Geochimica et Cosmochimica Acta, 54, 1353-1357.

Solis, R. P., Ramos-Candelaria, M. N., Maturgo O. O., Fragata, J. J., Ramos, S.G., 1998. Migration of high Cl/B molar ratio, gas depleted and cooler Masakrot fluids towards the Central Palayang Bayan sector of the Bacman Geothermal Production Field, Philippines. Proceedings, PNOC-EDC Geothermal Conference. Manila, Philippines, pp. 311-318.

Sussman, D., Javellana, S. P., Benavidez, P. J., 1993. Geothermal energy development in the Philippines: an overview. Geothermics, 22(5), 353-367.

Tebar, H. J., 1988. Petrology and Geochemistry of Pocdol Mountains, Sorsogon, Philippines. Master of Science in Geology Thesis, University of Canterbury. Christchurch, New Zealand.

Vennemann, T. W., O'Neil, J. R., 1996. Hydrogen isotope exchange reactions between hydrous minerals and molecular hydrogen: I. A new approach for the determination of hydrogen isotope fractionation at moderate temperatures. Geochimica et Cosmochima Acta, 60, 2437-2451.

Villacorte, J. D., Colina, R. N., Marquez, S. L., Sta Ana, F. X. M., 2015. An Update on the 3D Numerical Model of the Bacon-Manito Geothermal Field. Proceedings 2015 World Geothermal Congress, Melbourne, Australia.

Zaide-Delfin, M. C., Bueza, E. L., Reyes, A. G., Tebar, H. J., 1989. BACMAN II Resource Assessment. Technical Report, PNOC-EDC.

Zen, A., Hammarstrom, J., 1984. Magmatic epidote and its petrologic significance. Geology, 12(9), 515-518.

Zheng, Y. F., 1993. Calculation of oxygen isotope fractionation in hydroxyl-bearing silicates. Earth Planetary Science Letters, 120, 247-263.

Figure Captions

Figure 1. Location map of the Bacman geothermal field in the Pocdol Mountains, showing the different sectors: Palayang Bayan, Botong, Cawayan, Tanawon, Rangas, and Kayabon. The diagonal line represents a profile section of the field in Figure 10.

Figure 2. Backscattered electron image of a ~~grain sample~~cutting from PAL30D at a depth of 1700 m, measured depth (mMD). Euhedral epidote (ep) crystals register a lighter grey color in contrast to the dark gray calcite (ct)~~ mineral~~. There is also a noticeable brightness difference in the ~~color within~~ epidote grains due to compositional zoning, where the mineral interior is darker and more Al-rich compared to the rims which are lighter and more Fe-rich.

Figure 3. ~~Compositional electron microprobe data of~~Epidote compositions (FeO, SiO_2, CaO, and Al_2O_3) ~~in epidotes~~ from selected depths ~~of~~ for wells PAL18D, PAL30D, RS1D, and PAL8RD. The black diamonds ~~points are~~ representative average compositionsal ~~values from all epidotes analyzed in the same sampling depth~~at a given depth. Depths are expressed in m, measured depth (mMD).

Figure 4. Baseline (a) and updated (b) iso-Cl/B compositions of discharge fluids across different sectors in the Bacman geothermal reservoir. Baseline contours were generated from the data provided by Ruaya et al. (1993), while updated contours were generated from the data in this study.

Figure 5. Baseline (a) and updated (b) iso-$\delta^{18}O_{res}$ compositions of discharge fluids across different sectors in the Bacman geothermal reservoir. Baseline contours were generated from the data provided by Ruaya et al. (1993), while updated contours were generated from the data in this study.

Figure 6. (a) Fe-Al mole fraction and oxide ratio, and (b) MgO versus~~s.~~ depth ~~from~~ for PAL8RD ~~samples~~cuttings. The gray ~~datasets~~ symbols correspond to ~~XRF data~~whole rock compositions from cuttings and the black ~~datasets~~ symbols correspond to ~~representative electron microprobe data from~~ epidote mineral chemistry~~s~~. Compositions are in weight percent oxide, while depths are expressed in mMD.

Figure 7. δD vs. $\delta^{18}O$ plot of well fluid and epidote ~~samples~~ from the Bacman geothermal system, Philippines. Gray ~~data points~~symbols refer to well fluid compositions from this study (see Supplemental Table 4), while the ~~elongated field~~ delineated field ~~by a dotted line~~ represents baseline well fluid compositions from Ruaya et al. (1993). The black cross corresponds to representative local meteoric waters (δD = -24.7 ‰ and δ18O = -4.8 ‰) from Salonga (2015).

Figure 8. D/H (from Chacko et al., 1999) vs. $^{18}O/^{16}O$ (from Pope et al., 2016) isotope fractionation values between epidote and fluid as a function of temperature. The plotted values ~~plotted were obtained from~~ are the difference in ~~the~~ isotopic composition of epidote~~s~~ and well discharges. ~~The~~

~~numbers beside the data points correspond to the depths~~Sample depth in mMD is indicated next to each symbol ~~of the samples~~. The black line delineates the isotopic equilibrium with respect to the isotope fractionation ~~values~~ for both D/H and $^{18}O/^{16}O$ as a function of temperature. The vertical and horizontal gray fields ~~are~~ delineat~~ed from~~ the temperature range where epidotes typically occur in geothermal systems, and the corresponding isotope fractionation ~~values~~ for both D/H and $^{18}O/^{16}O$.

Figure 9. Reservoir $\delta^{18}O$ vs. ~~reservoir chloride~~Cl_{res} ~~plot of~~for selected Bacman wells. Filled data points represent ~~the natural state~~baseline chemistry prior to production (~~baseline data, from~~ Ruaya et al., 1993), while ~~unfilled data~~open symbols ~~points~~ represent the production state of the field (data from this study). Arrows indicate compositional changes ~~movement of data points~~ through time, ~~which are~~ caused by particular reservoir processes as discussed in the text.

Figure 10. Profile section of the Bacman geothermal field showing the updated hydrogeological model of the ~~geothermal~~ reservoir which now includes the Rangas and Kayabon sectors. Fluid mixing and water-rock interaction are regarded as the two-most important reservoir processes that have influenced the evolution of Bacman reservoir fluids. Up ~~or~~/ down arrows next to $\delta^{18}O$ or δD indicate the corresponding respective increase or decrease in the isotopic composition of the resulting fluid due to each dominant reservoir process. Refer to Figure 1 for the transect line. Profile not drawn to scale.

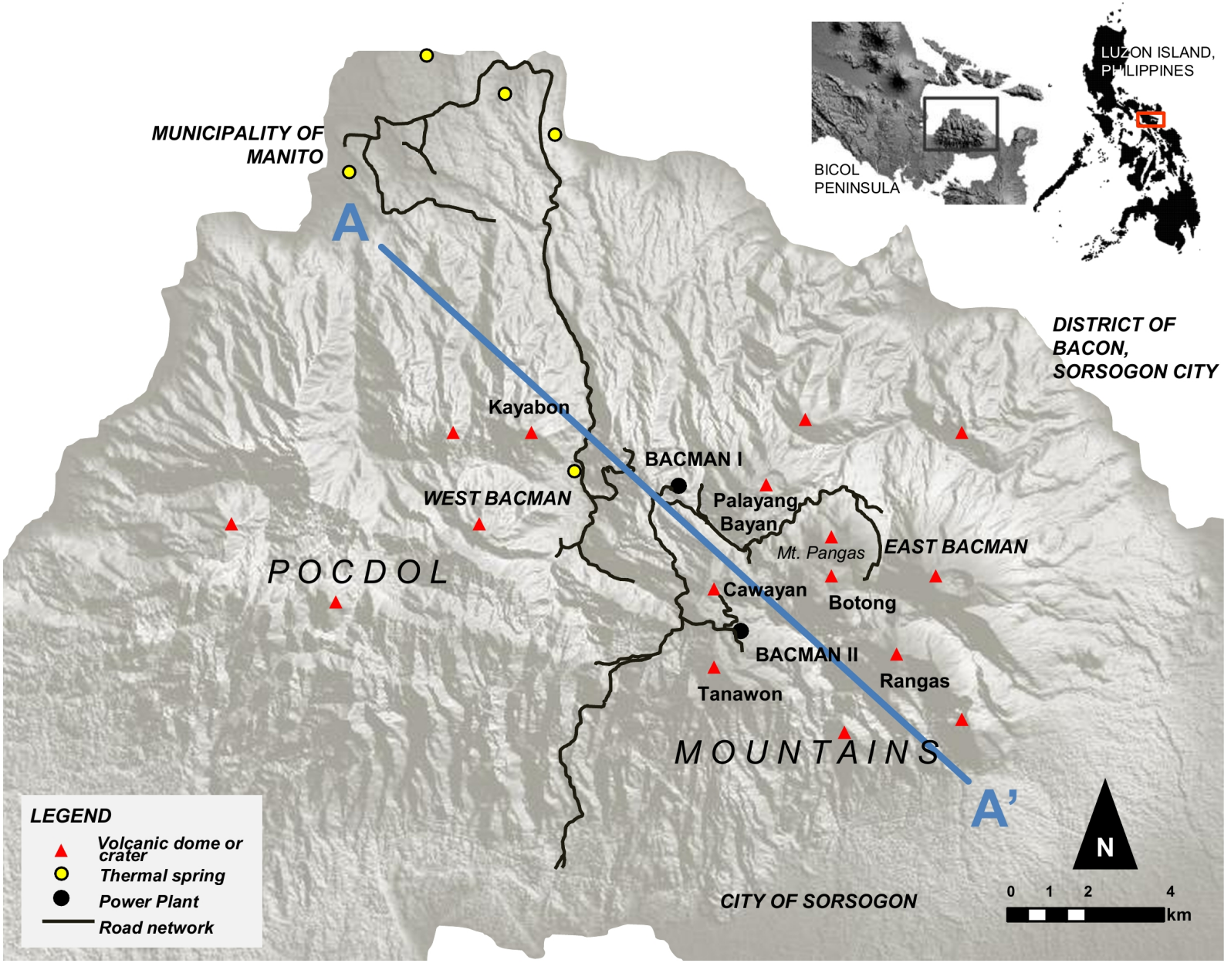
MUNICIPALITY OF MANITO
A
A'
DISTRICT OF BACON, SORSOGON CITY
LUZON ISLAND, PHILIPPINES
BICOL PENINSULA
Kayabon
BACMAN I
WEST BACMAN
Palayang Bayan
Mt. Pangas
EAST BACMAN
POCDOL
Cawayan
Botong
BACMAN II
Rangas
Tanawon
MOUNTAINS
CITY OF SORSOGON
N
0 1 2 4
km
LEGEND
Volcanic dome or crater
Thermal spring
Power Plant
Road network

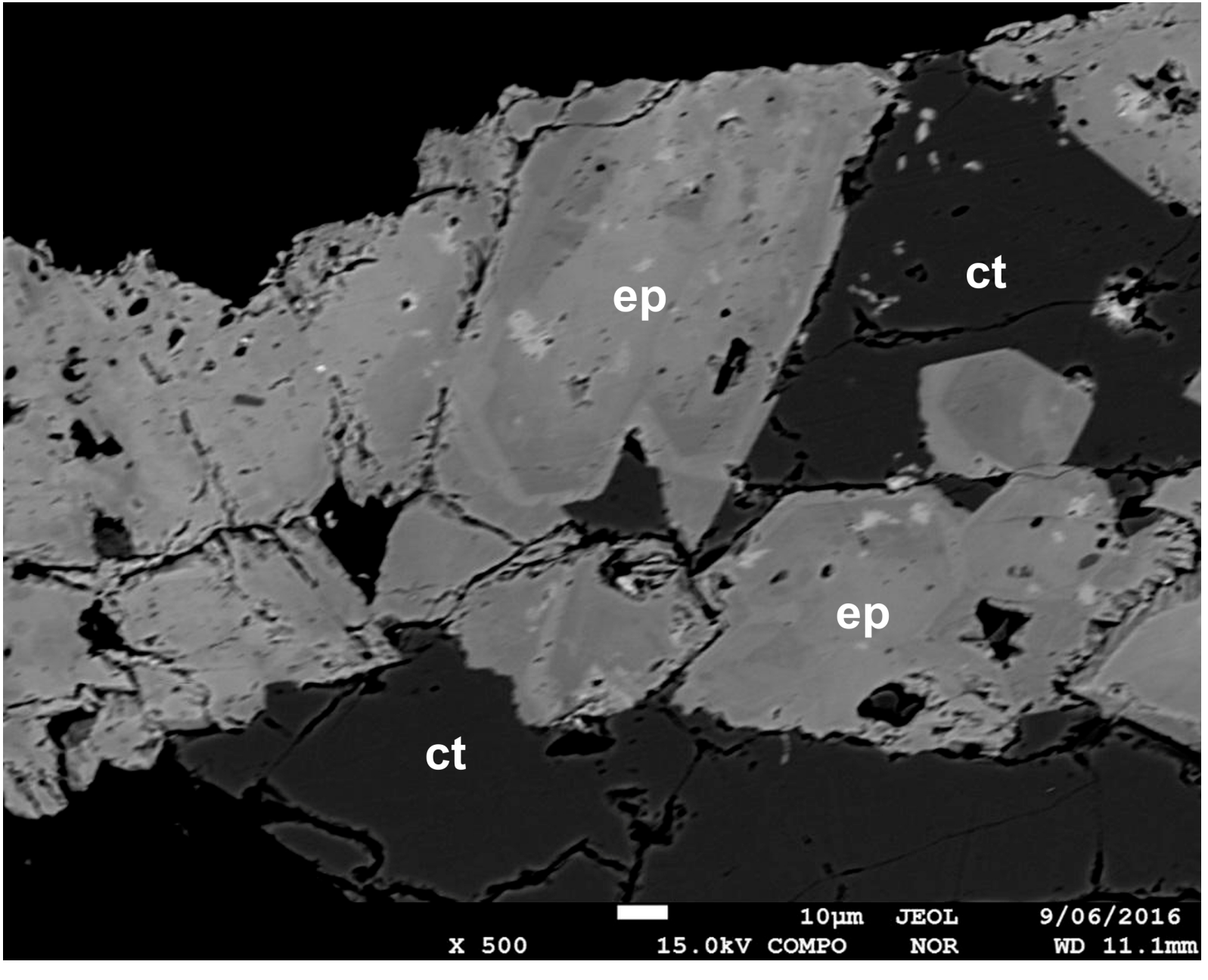
ep
ct
ep
ct
10µm JEOL 9/06/2016
X 500 15.0kV COMPO NOR WD 11.1mm

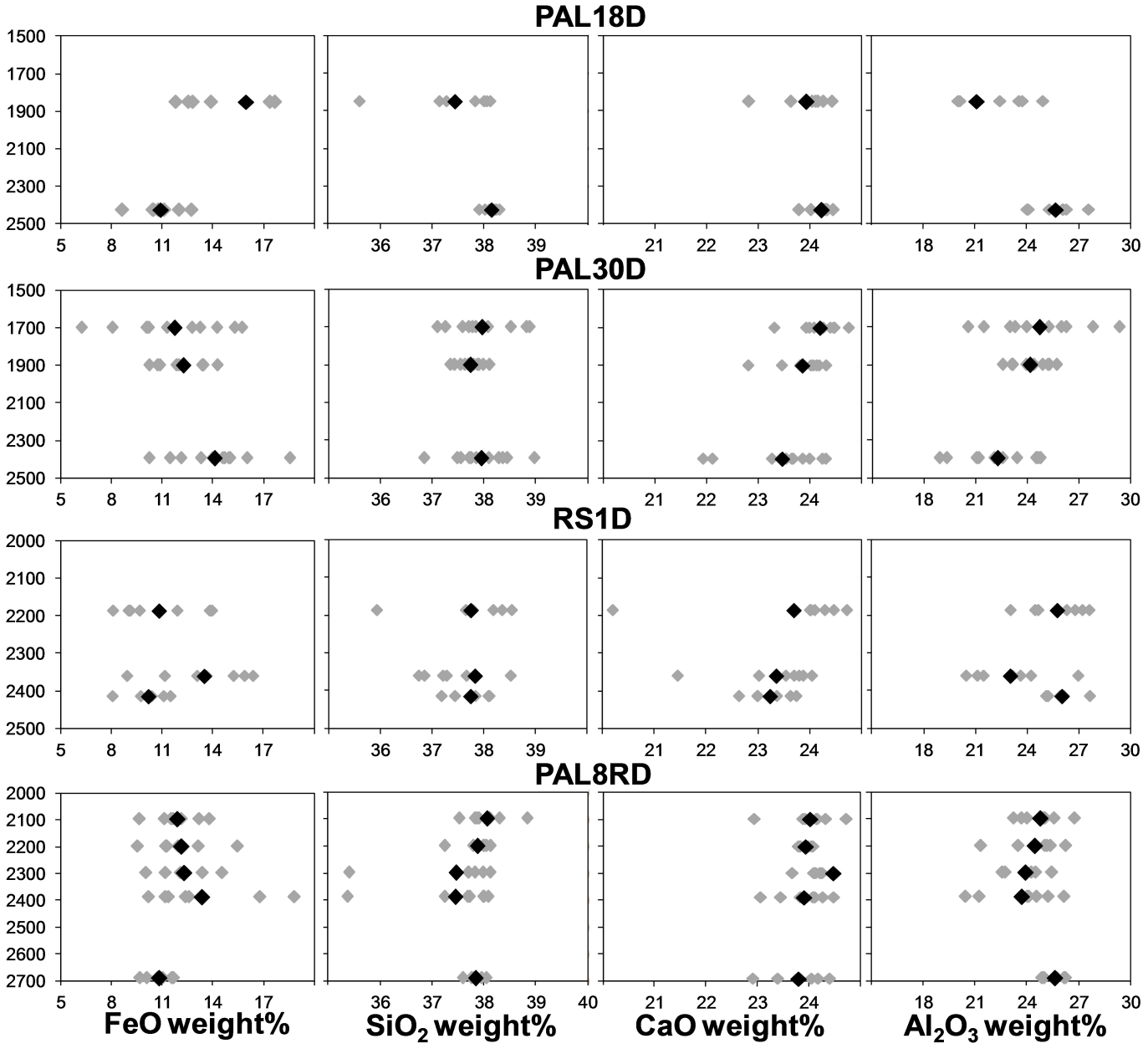
PAL18D
PAL30D
RS1D
PAL8RD
FeO weight%
SiO2 weight%
CaO weight%
Al2O3 weight%

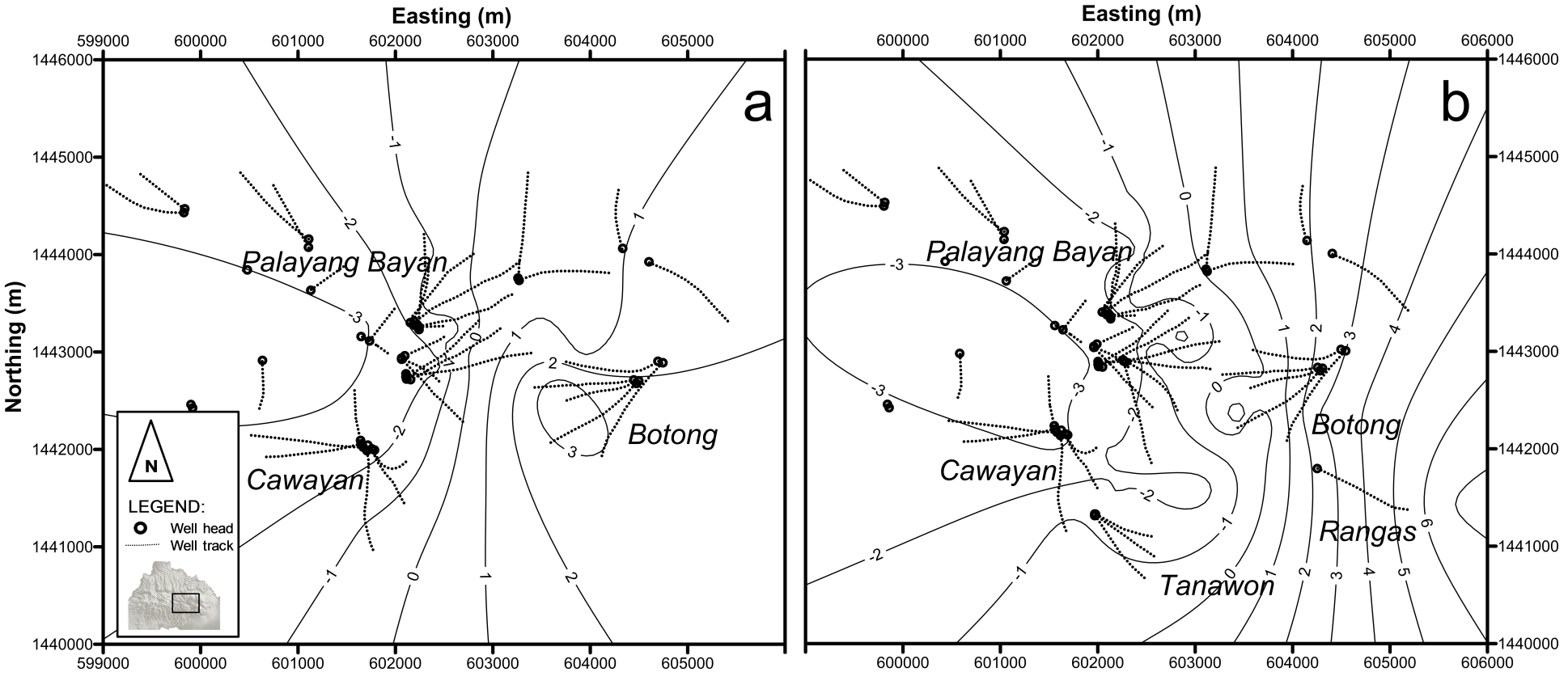
a
b
Easting (m)
Northing (m)
Palayang Bayan
Cawayan
Botong
Tanawon
Rangas
N
LEGEND:
Well head
Well track

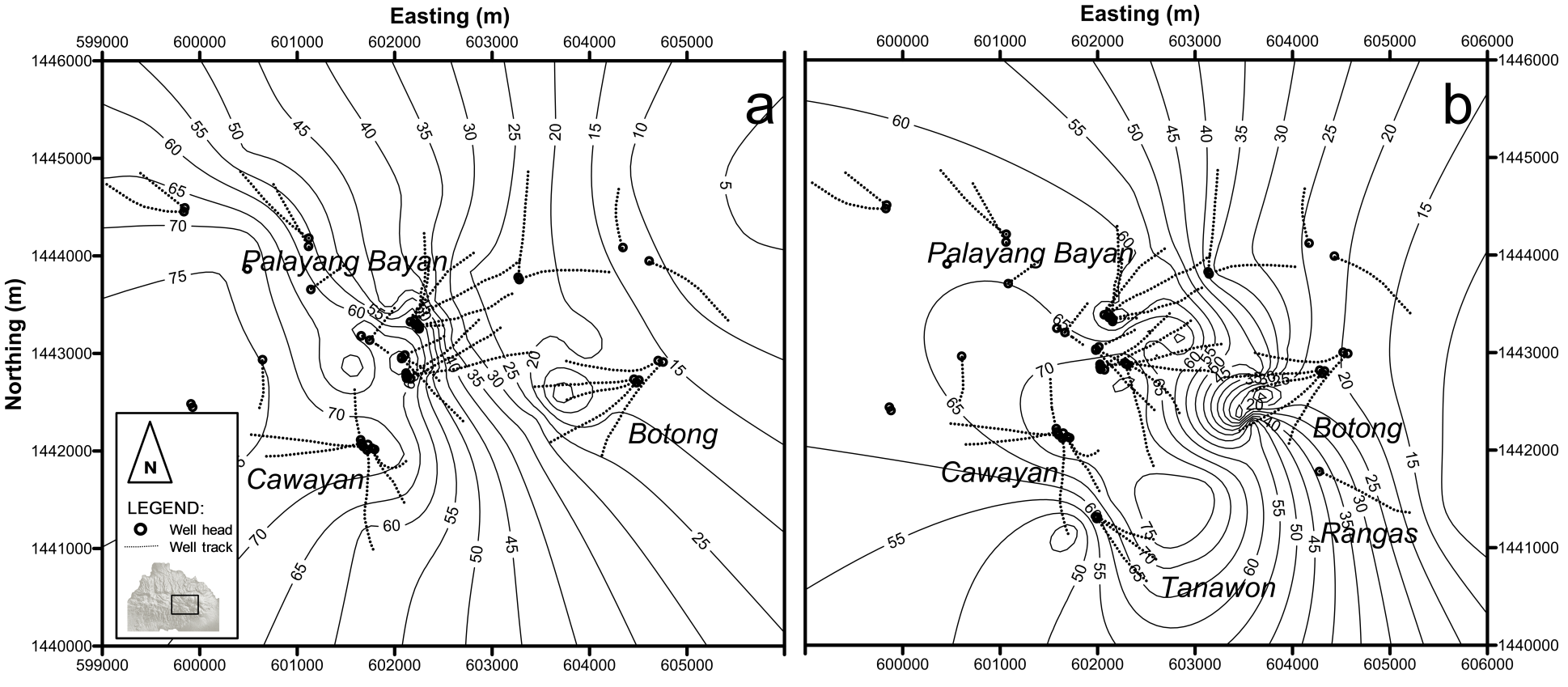
a
b
Easting (m)
Northing (m)
Palayang Bayan
Cawayan
Botong
Tanawon
Rangas
N
LEGEND:
Well head
Well track

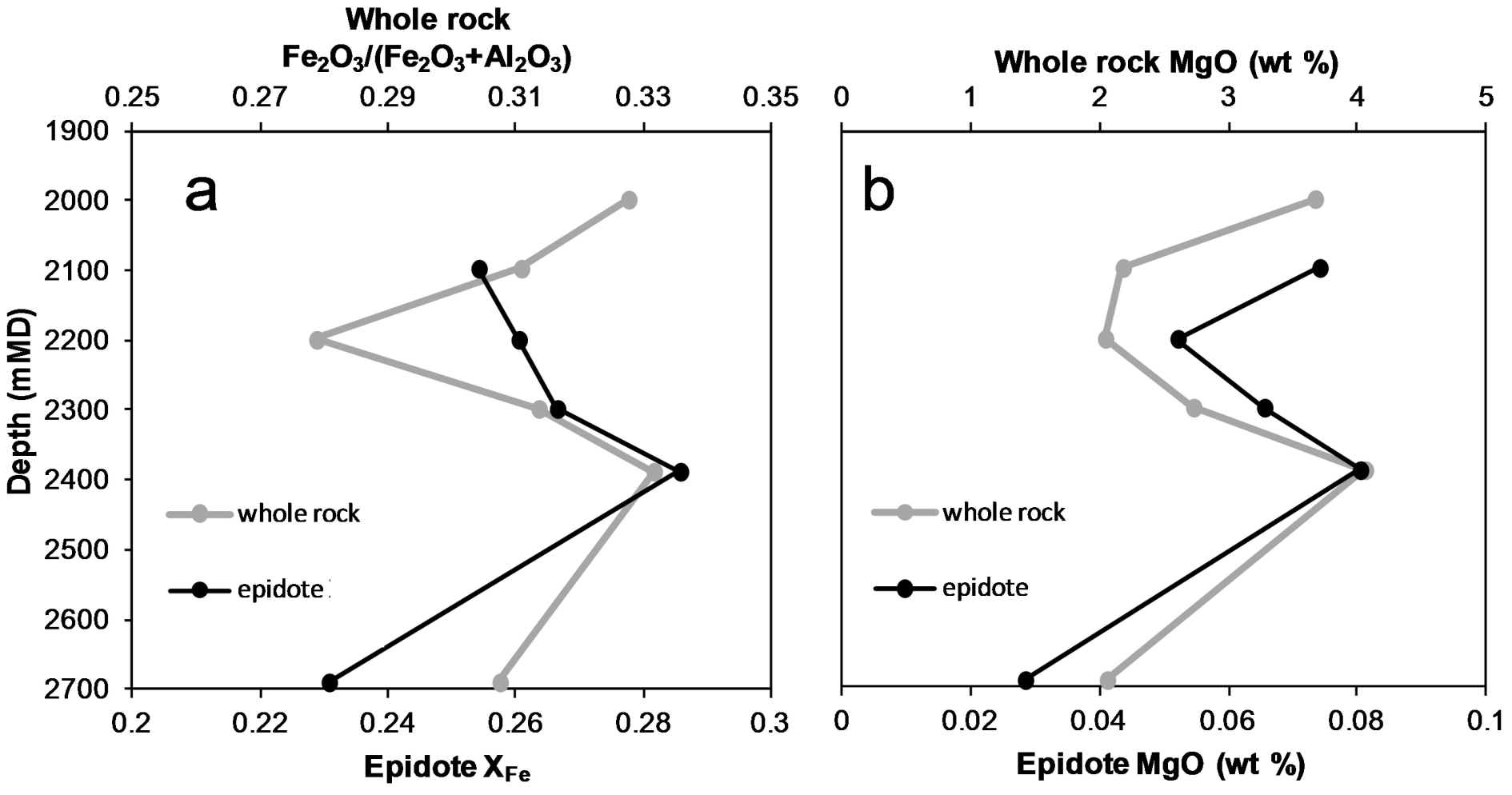
Whole rock
Fe2O3/(Fe2O3+Al2O3)
0.25
0.27
0.29
0.31
0.33
0.35
1900
2000
2100
2200
2300
2400
2500
2600
2700
Depth (mMD)
a
whole rock
epidote
0.2
0.22
0.24
0.26
0.28
0.3
Epidote XFe
Whole rock MgO (wt %)
0
1
2
3
4
5
b
whole rock
epidote
0
0.02
0.04
0.06
0.08
0.1
Epidote MgO (wt %)

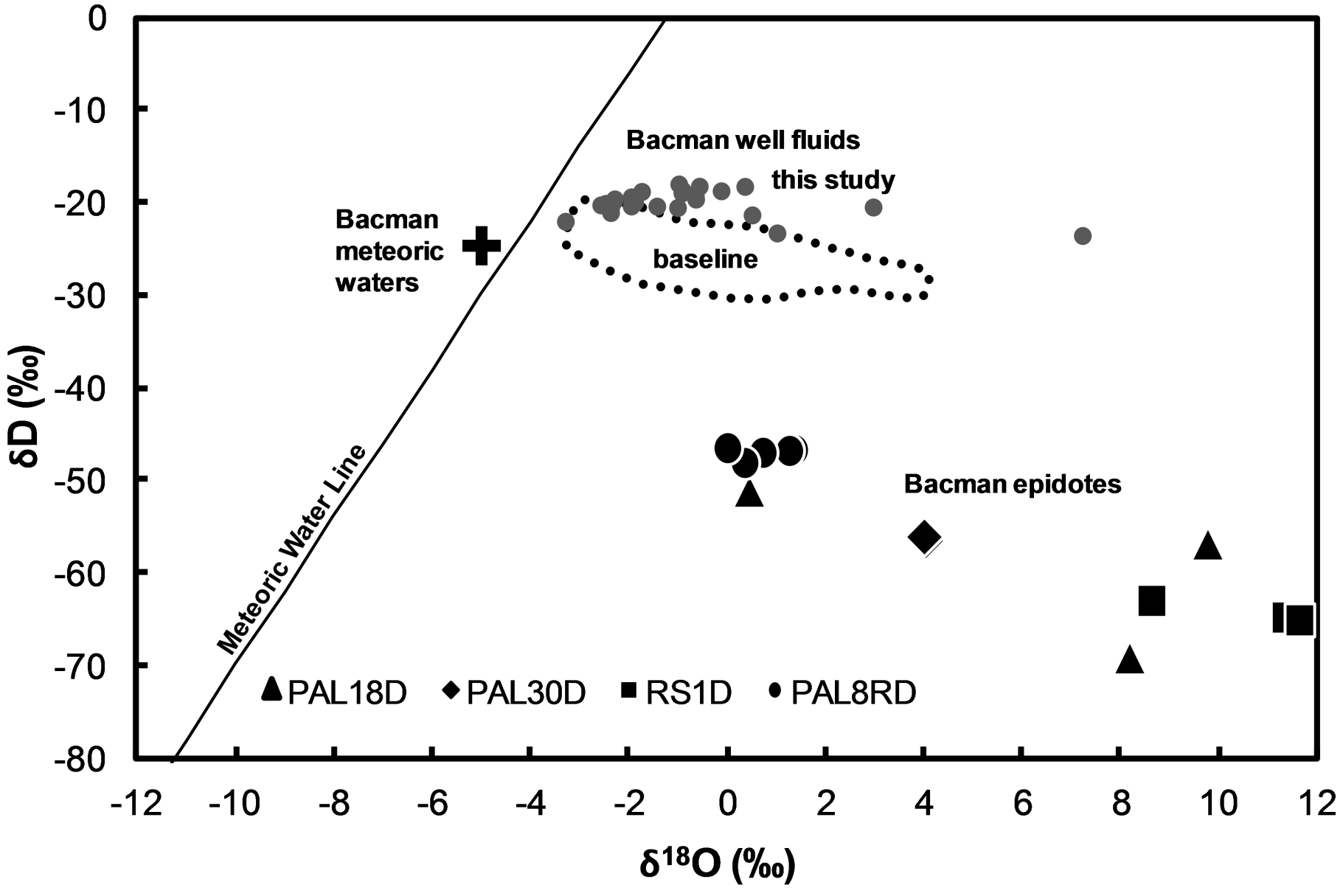
Bacman well fluids
this study
Bacman meteoric waters
baseline
Meteoric Water Line
Bacman epidotes
PAL18D
PAL30D
RS1D
PAL8RD
δD (‰)
δ18O (‰)
0
-10
-20
-30
-40
-50
-60
-70
-80
-12
-10
-8
-6
-4
-2
0
2
4
6
8
10
12

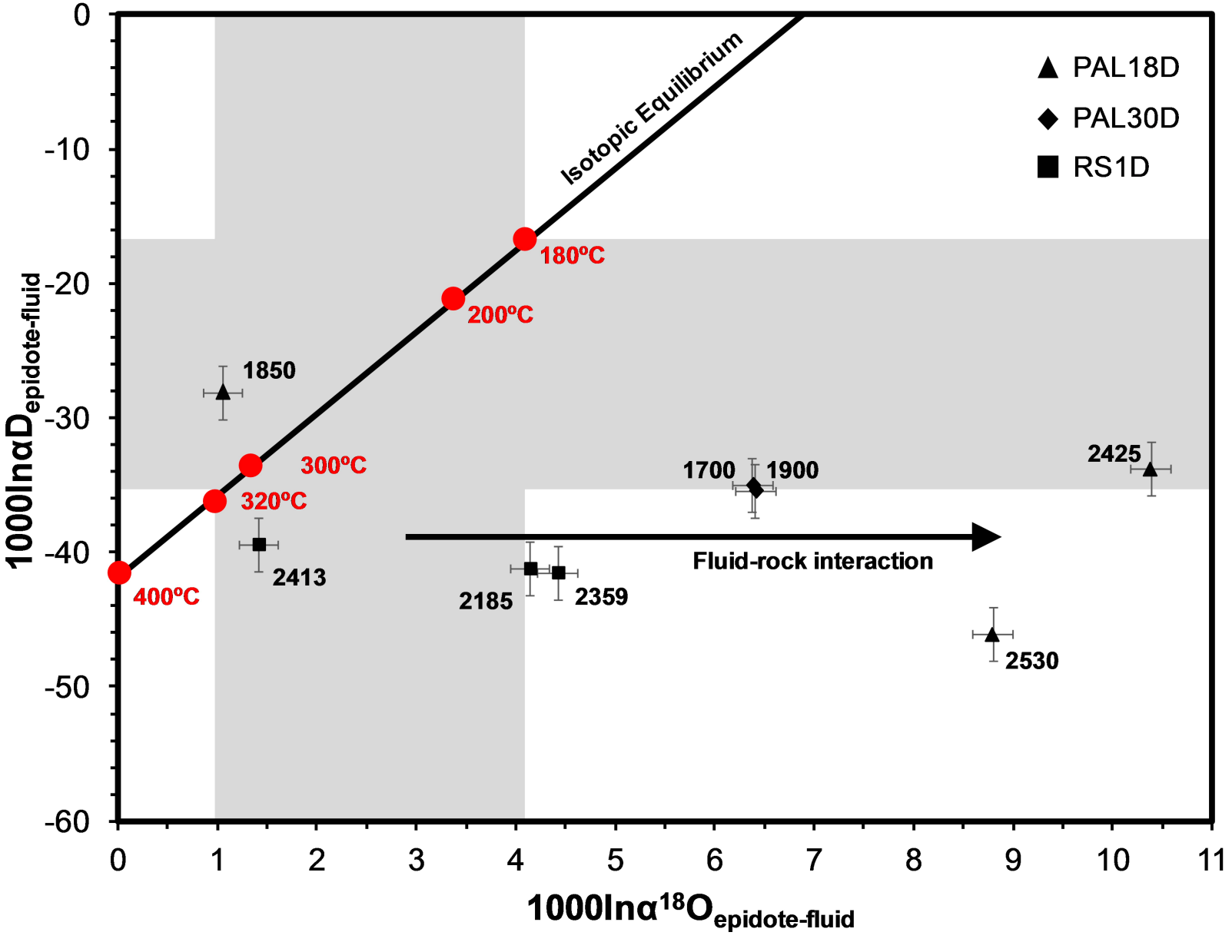
PAL18D
PAL30D
RS1D
Isotopic Equilibrium
180ºC
200ºC
300ºC
320ºC
400ºC
1850
2413
2185
2359
1700
1900
2425
2530
Fluid-rock interaction
1000lnαD epidote-fluid
1000lnα18O epidote-fluid
0
-10
-20
-30
-40
-50
-60
0
1
2
3
4
5
6
7
8
9
10
11

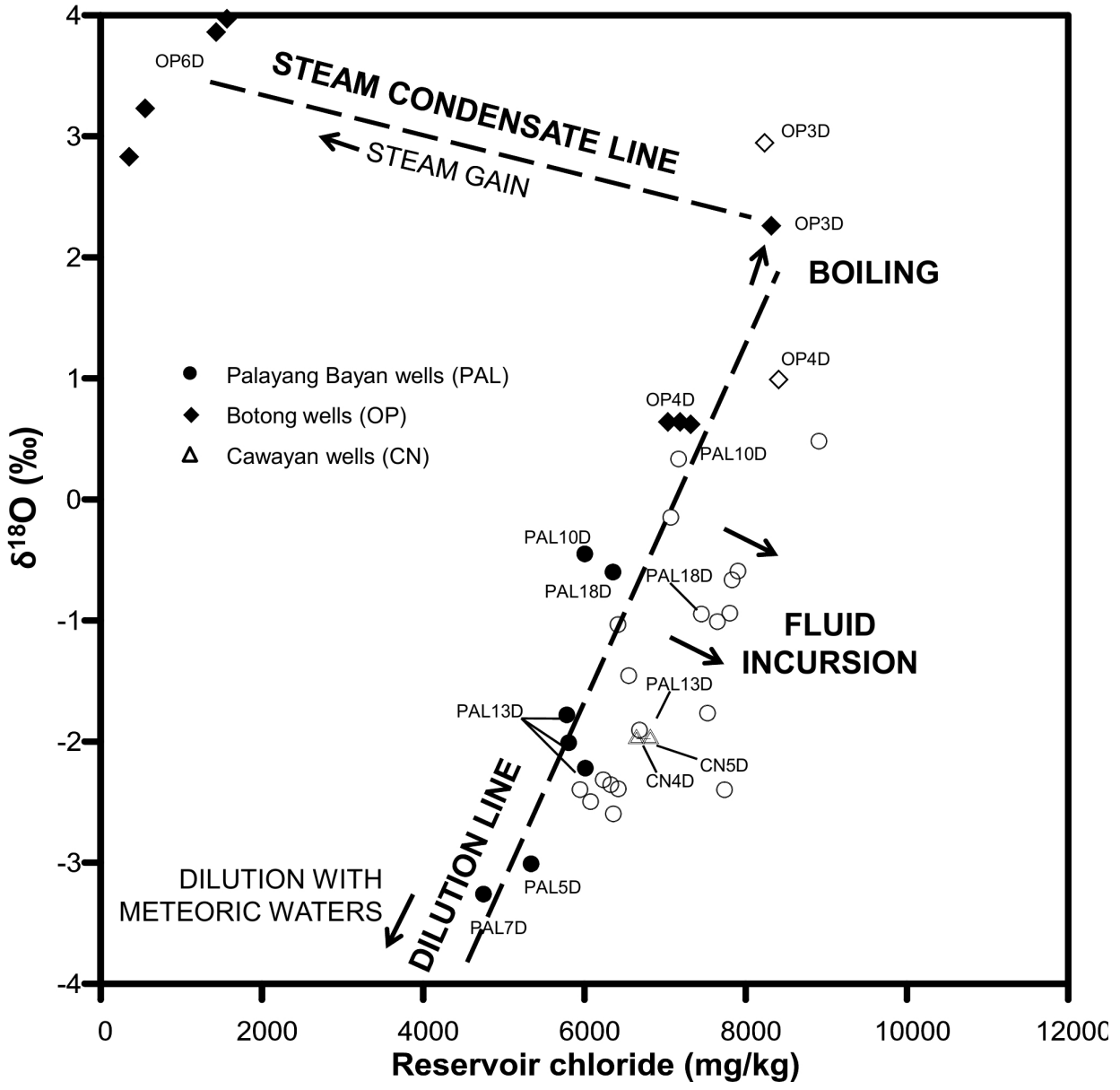
STEAM CONDENSATE LINE
STEAM GAIN
BOILING
FLUID INCURSION
DILUTION LINE
DILUTION WITH METEORIC WATERS
Palayang Bayan wells (PAL)
Botong wells (OP)
Cawayan wells (CN)
OP6D
OP3D
OP3D
OP4D
OP4D
PAL10D
PAL10D
PAL18D
PAL18D
PAL13D
PAL13D
CN5D
CN4D
PAL5D
PAL7D
δ18O (‰)
Reservoir chloride (mg/kg)
4
3
2
1
0
-1
-2
-3
-4
0
2000
4000
6000
8000
10000
12000

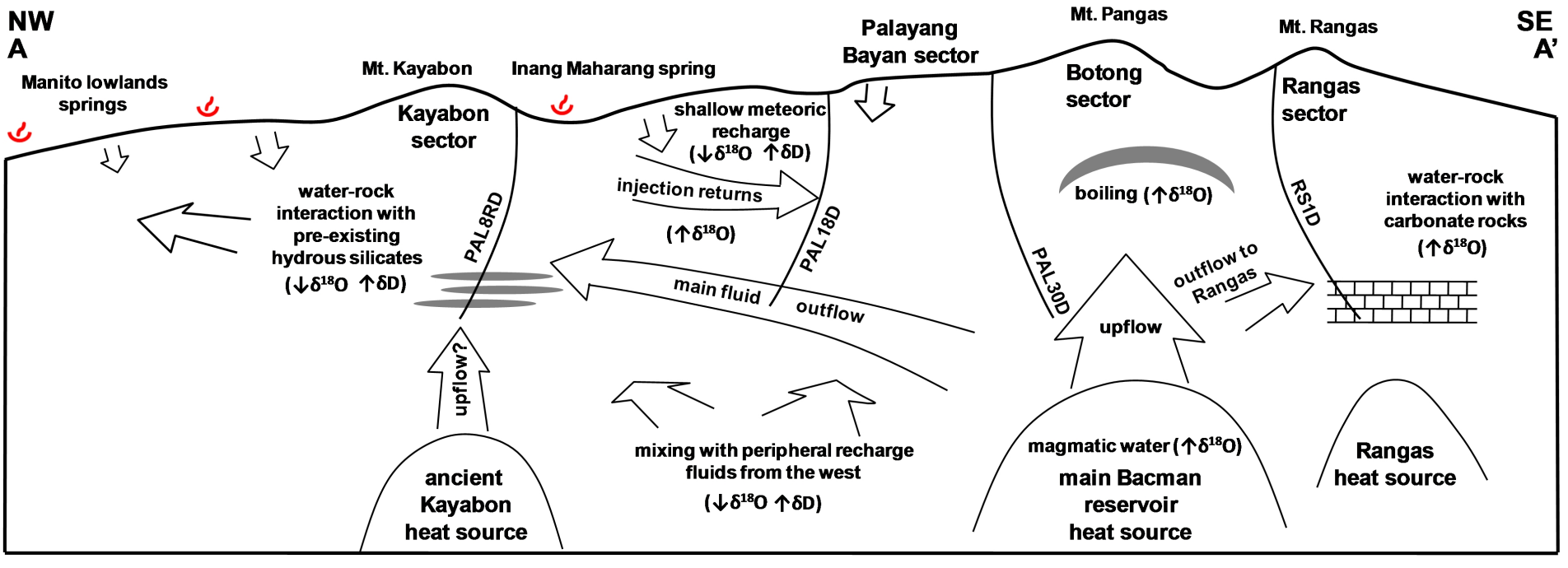
NW
A
SE
A'
Manito lowlands springs
Mt. Kayabon
Inang Maharang spring
Palayang Bayan sector
Mt. Pangas
Mt. Rangas
Kayabon sector
Botong sector
Rangas sector
shallow meteoric recharge (↓δ18O ↑δD)
injection returns
(↑δ18O)
boiling (↑δ18O)
water-rock interaction with pre-existing hydrous silicates (↓δ18O ↑δD)
PAL8RD
PAL18D
PAL30D
RS1D
water-rock interaction with carbonate rocks (↑δ18O)
main fluid
outflow
outflow to Rangas
upflow
upflow?
mixing with peripheral recharge fluids from the west
(↓δ18O ↑δD)
magmatic water (↑δ18O)
main Bacman reservoir heat source
ancient Kayabon heat source
Rangas heat source

Table 1. Whole rock and alteration mineralogy of borehole samples, and corresponding δD and $\delta^{18}O$ isotopic composition of reservoir fluids from discharge data, epidotes, and fluids in equilibrium with epidote ($\delta D_{fluid(eq)}$, $\delta^{18}O_{fluid(eq)}$).

Well	Depth	Elevation	Whole rock Lithology	Dominant Alteration Mineralogy	Discharge fluid (δ_{fluid})		Epidote		Fluid in equilibrium with epidote ($\delta_{fluid(eq)}$)		
	mMD	mRSL			δD	$\delta^{18}O$	δD	$\delta^{18}O$	Temperature (°C)	$\delta D_{fluid(eq)}$	$\delta^{18}O_{fluid(eq)}$
PAL18D	1850	-1012	porphyritic andesite	chlorite, epidote	-23.0*	-0.6*	-51.1	+0.5	277	-19.9	-1.3
	2425	-1518	micordiorite	epidote, chlorite			-56.8	+9.8	276	-25.8	+8.0
	2530	-1620	microdiorite	tremolite/actinolite, chlorite, epidote			-69.1	+8.2	271	-38.6	+6.3
PAL30D	1700	-850	porphyritic andesite	epidote	-21.0	-2.4	-56.4	+4.0	257	-27.6	+1.9
	1900	-1010	porphyritic andesite	epidote, tremolite/ actinolite			-56.0	+4.0	261	-26.7	+1.9
	2395	-1442	sedimentary breccia	tremolite/actinolite, chlorite, epidote			-	+4.5	242	-	+2.1
RS1D	2185	-1353	calcareous sedimentary breccia, limestone	calcite, epidote, tremolite/actinolite	-23.5	+7.2	-64.7	+11.3	295	-31.6	+9.9
	2359	-1498	fossiliferous limestone, minor porphyritic andesite	calcite, epidote, wairakite/ laumontite, chlorite			-65.0	+11.6	301	-31.3	+10.3
	2413	-1544	calcareous sedimentary breccia	calcite, epidote, tremolite/actinolite			-62.9	+8.6	292	-30.1	+7.1
PAL8RD	2097	-1542	tuffaceous volcanic breccia	chlorite, epidote, illite, tremolite/ actinolite	-	-	-46.6	+1.3	-	-	-
	2199	-1618	tuffaceous volcanic breccia	epidote, chlorite, illite, tremolite/ actinolite			-46.7	+1.2	-	-	-
	2298	-1693	tuffaceous volcanic breccia	epidote, chlorite, tremolite/actinolite			-46.9	+0.7	-	-	-
	2388	-1761	tuffaceous volcanic breccia	epidote, wairakite/ laumontite, chlorite			-48.0	+0.3	-	-	-
	2690	-1990	porphyritic andesite	epidote, quartz, wairakite/laumontite			-46.4	0.0	244	-19.3	-2.4

*Baseline isotopic composition of PAL18D obtained from Ruaya et al. (1993).

Depth and elevation are expressed in mMD (meters, measured depth) and mRSL (meters, relative to sea level), respectively. The $\delta D_{fluid(eq)}$ and $\delta^{18}O_{fluid(eq)}$ values were calculated using Equations 2 and 3 given the isotopic data from discharge fluids and downhole temperature. The δD and $\delta^{18}O$ values for each well were applied to every depth. Temperature values were obtained from downhole measurements from EDC, except for PAL8RD temperature which was obtained from fluid inclusion homogenization temperature estimates from Doma (2015).

Table 2. Representative data from electron microprobe analysis of epidotes.

WELL	Depth	Weight Percent (%)										
		TiO_2	CaO	Na_2O	MgO	SiO_2	Al_2O_3	MnO	Cr_2O_3	FeO	Cl	Total
PAL18D	1850	0.05	23.93	0.005	0.039	37.44	21.08	0.11	0.009	15.94	0.002	98.60
	2425	0.18	24.22	0.008	0.053	38.14	25.65	0.29	0.009	10.90	0.003	99.45
PAL30D	1700	0.13	24.20	0.004	0.024	37.95	24.72	0.20	0.015	11.74	0.003	98.99
	1900	0.07	23.86	0.004	0.056	37.73	24.17	0.42	0.019	12.26	0.007	98.58
	2395	0.01	23.47	0.021	0.556	37.94	22.29	0.16	0.013	14.11	0.017	98.58
RS1D	2185	0.05	23.69	0.008	0.326	37.73	25.74	0.09	0.015	10.82	0.008	98.48
	2359	0.00	23.35	0.154	0.090	37.81	23.02	0.11	0.010	13.49	0.025	98.06
	2413	0.05	23.23	0.010	0.055	37.73	26.01	0.10	0.020	10.19	0.003	97.41
PAL8RD	2097	0.05	24.02	0.067	0.074	38.06	24.77	0.30	0.025	11.88	0.005	99.24
	2199	0.12	23.93	0.011	0.052	37.87	24.45	0.46	0.005	12.12	0.003	99.04
	2298	0.03	24.47	0.011	0.063	37.46	23.91	0.24	0.019	12.28	0.003	98.49
	2388	0.09	23.90	0.009	0.080	37.45	23.70	0.21	0.015	13.34	0.003	98.80
	2690	0.05	23.79	0.003	0.028	37.84	25.62	0.48	0.027	10.81	0.001	98.65

WELL	Depth	Cations per 12.5 Anhydrous Oxygens									
		Ti	Ca	Na	Mg	Si	Al	Mn	Cr	Fe	X_{Fe}
PAL18D	1850	0.003	2.118	0.001	0.005	3.093	2.049	0.007	0.001	1.101	0.349
	2425	0.010	2.063	0.001	0.006	3.032	2.399	0.020	0.001	0.724	0.232
PAL30D	1700	0.008	2.081	0.001	0.003	3.047	2.335	0.014	0.001	0.788	0.252
	1900	0.004	2.068	0.001	0.007	3.053	2.301	0.029	0.001	0.829	0.265
	2395	0.001	2.052	0.003	0.068	3.096	2.140	0.011	0.001	0.962	0.310
RS1D	2185	0.003	2.034	0.001	0.039	3.024	2.427	0.006	0.001	0.724	0.230
	2359	0.000	2.044	0.024	0.011	3.090	2.213	0.008	0.001	0.921	0.294
	2413	0.003	2.006	0.001	0.007	3.042	2.467	0.007	0.001	0.687	0.218
PAL8RD	2097	0.003	2.062	0.010	0.009	3.049	2.335	0.020	0.002	0.795	0.254
	2199	0.007	2.063	0.002	0.006	3.047	2.315	0.031	0.000	0.815	0.260
	2298	0.002	2.129	0.002	0.008	3.041	2.283	0.016	0.001	0.833	0.267
	2388	0.005	2.080	0.001	0.010	3.041	2.264	0.015	0.001	0.905	0.286
	2690	0.003	2.043	0.001	0.003	3.032	2.415	0.033	0.002	0.724	0.231

Sample depths are in meters, measured depth (mMD). Total Fe expressed as FeO.

AUTHOR DECLARATION

We wish to draw the attention of the Editor to the following facts which may be considered as potential conflicts of interest and to significant financial contributions to this work.

First author Julius Dimabayao was funded to conduct research presented in this manuscript as part of his MSc at the University of Auckland on the Bacon-Manito Geothermal Field (Bacman) by Energy Development Corporation (EDC) and is an employee of the EDC. Interpretations were developed independent of EDC input as independent research at the University of Auckland and therefore we do not feel there is a significant conflict of interest here.

We confirm that the manuscript has been read and approved by all named authors and that there are no other persons who satisfied the criteria for authorship but are not listed. We further confirm that the order of authors listed in the manuscript has been approved by all of us.

We confirm that we have given due consideration to the protection of intellectual property associated with this work and that there are no impediments to publication, including the timing of publication, with respect to intellectual property. In so doing we confirm that we have followed the regulations of our institutions concerning intellectual property.

We understand that the Corresponding Author is the sole contact for the Editorial process (including Editorial Manager and direct communications with the office). He/she is responsible for communicating with the other authors about progress, submissions of revisions and final approval of proofs. We confirm that we have provided a current, correct email address which is accessible by the Corresponding Author and which has been configured to accept email from (Michael.rowe@auckland.ac.nz).

Signed by all authors as follows:

Dr. Michael Rowe (on behalf of co-authors) 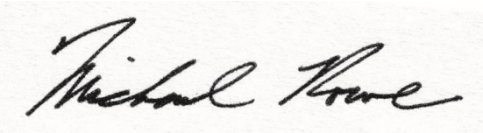 June 30, 2018

~~SUPPLEMENTARY~~ SUPPLEMENTAL TABLES

~~Supplementary~~ Supplemental Table 1: Full dataset of electron microprobe analysis of epidotes from four Bacman wells.

WELL	Depth	Weight Percent (%)										
		TiO_2	CaO	Na_2O	MgO	SiO_2	Al_2O_3	MnO	Cr_2O_3	FeO	Cl	Total
PAL18D	1850	0.002	24.27	0.000	0.044	37.83	22.46	0.096	0.000	13.90	0.003	98.60
	1850	0.102	23.64	0.007	0.063	37.15	20.04	0.117	0.000	17.38	0.003	98.50
	1850	0.058	22.82	0.004	0.020	35.61	12.68	0.133	0.000	25.42	0.000	96.75
	1850	0.025	24.44	0.008	0.053	38.12	24.94	0.094	0.009	11.82	0.005	99.51
	1850	0.020	24.16	0.000	0.031	38.01	23.75	0.118	0.027	12.56	0.000	98.68
	1850	0.001	24.12	0.000	0.032	38.06	23.56	0.139	0.030	12.82	0.003	98.76
	1850	0.143	24.05	0.016	0.027	37.28	20.15	0.052	0.000	17.68	0.001	99.40
	2425	0.299	24.28	0.014	0.079	38.18	24.10	0.000	0.000	12.74	0.003	99.70
	2425	0.050	24.34	0.008	0.037	38.11	26.14	0.335	0.000	10.78	0.004	99.80
	2425	0.531	24.46	0.000	0.074	38.02	24.03	0.151	0.046	12.01	0.003	99.33
	2425	0.009	23.79	0.008	0.033	38.25	26.30	0.607	0.000	10.46	0.006	99.47
	2425	0.001	24.03	0.023	0.042	38.30	26.08	0.387	0.000	10.51	0.003	99.38
	2425	0.266	24.33	0.000	0.050	37.91	25.32	0.285	0.018	11.14	0.000	99.31
	2425	0.075	24.32	0.000	0.054	38.22	27.58	0.281	0.000	8.65	0.001	99.18
PAL30D	1700	0.000	24.00	0.000	0.033	37.70	23.02	0.148	0.018	14.27	0.000	99.19
	1700	0.075	24.23	0.000	0.020	38.07	26.29	0.205	0.009	10.23	0.000	99.13
	1700	0.020	24.27	0.007	0.013	37.77	25.27	0.217	0.000	11.31	0.000	98.88
	1700	0.160	24.47	0.000	0.026	37.09	21.50	0.016	0.018	15.31	0.015	98.61
	1700	0.076	24.49	0.007	0.016	38.82	27.84	0.114	0.052	8.09	0.000	99.50
	1700	0.023	24.76	0.018	0.007	38.88	29.38	0.019	0.009	6.27	0.002	99.37
	1700	0.000	23.32	0.003	0.019	37.58	23.99	0.666	0.000	13.27	0.001	98.85
	1700	0.093	24.09	0.000	0.029	37.84	23.32	0.172	0.030	12.79	0.005	98.36
	1700	0.013	24.41	0.000	0.014	38.51	26.01	0.239	0.015	10.10	0.000	99.31
	1700	0.846	23.94	0.000	0.066	37.25	20.59	0.230	0.000	15.75	0.003	98.67
	1900	0.000	23.82	0.000	0.058	37.42	22.61	0.587	0.021	14.30	0.003	98.81
	1900	0.102	23.47	0.000	0.046	37.62	24.41	0.703	0.030	12.22	0.006	98.60
	1900	0.000	23.88	0.004	0.075	37.87	24.92	0.285	0.036	12.01	0.004	99.09
	1900	0.130	22.82	0.001	0.029	37.90	25.74	1.429	0.000	10.27	0.000	98.32
	1900	0.137	24.19	0.000	0.016	37.98	25.30	0.196	0.000	10.90	0.005	98.72
	1900	0.001	24.07	0.012	0.078	37.54	23.19	0.237	0.027	13.39	0.013	98.56
	1900	0.014	24.03	0.000	0.092	37.79	23.17	0.219	0.024	13.46	0.013	98.82
	1900	0.174	24.32	0.003	0.017	38.10	25.23	0.127	0.003	10.76	0.004	98.74
	1900	0.001	24.14	0.016	0.067	37.69	23.97	0.186	0.009	11.87	0.018	97.96
	1900	0.146	23.83	0.000	0.083	37.35	23.13	0.214	0.036	13.42	0.004	98.20
	2395	0.000	22.12	0.022	2.888	38.44	18.95	0.207	0.033	14.72	0.020	97.40
	2395	0.000	23.55	0.001	0.417	38.36	22.38	0.063	0.003	14.01	0.010	98.80

WELL	Depth	Weight Percent (%)										
		TiO_2	CaO	Na_2O	MgO	SiO_2	Al_2O_3	MnO	Cr_2O_3	FeO	Cl	Total
RS1D	2185	0.082	24.10	0.006	0.014	38.53	27.23	0.052	0.031	9.04	0.005	99.10
	2185	0.028	24.47	0.000	0.075	37.78	26.32	0.120	0.009	9.70	0.011	98.51
	2185	0.045	24.73	0.017	0.035	38.35	27.63	0.047	0.003	8.12	0.008	98.98
	2185	0.055	24.03	0.000	0.039	37.73	24.67	0.075	0.003	11.92	0.004	98.52
	2185	0.000	24.01	0.003	0.033	37.65	23.06	0.073	0.018	13.84	0.005	98.68
	2185	0.131	24.30	0.000	0.031	38.18	26.81	0.028	0.043	9.14	0.003	98.66
	2185	0.031	20.19	0.033	2.052	35.92	24.48	0.207	0.000	13.97	0.020	96.91
	2359	0.000	21.45	1.014	0.114	40.48	24.25	0.059	0.000	11.18	0.010	98.55
	2359	0.000	23.71	0.003	0.048	36.73	20.48	0.101	0.000	16.40	0.014	97.48
	2359	0.000	23.55	0.007	0.048	37.20	23.17	0.322	0.000	13.64	0.006	97.94
	2359	0.020	24.05	0.000	0.041	38.51	26.98	0.099	0.027	8.96	0.007	98.69
	2359	0.007	23.80	0.000	0.154	37.66	23.64	0.078	0.000	13.09	0.005	98.43
	2359	0.000	23.88	0.022	0.171	37.28	21.49	0.000	0.000	15.25	0.000	98.08
	2359	0.002	23.02	0.029	0.055	36.84	21.13	0.110	0.042	15.90	0.136	97.24
	2413	0.045	23.64	0.016	0.065	38.10	25.99	0.130	0.040	10.41	0.006	98.44
	2413	0.024	23.00	0.005	0.055	37.83	26.14	0.092	0.000	10.23	0.004	97.38
	2413	0.045	22.99	0.012	0.054	38.08	27.66	0.026	0.000	8.09	0.002	96.97
	2413	0.075	22.64	0.000	0.054	37.17	25.12	0.134	0.000	11.12	0.004	96.32
	2413	0.128	23.75	0.011	0.063	37.43	25.94	0.071	0.012	9.77	0.004	97.17
	2413	0.010	23.37	0.013	0.039	37.76	25.23	0.172	0.067	11.52	0.000	98.18
PAL8RD	2097	0.014	23.94	0.000	0.025	37.91	25.59	0.446	0.000	11.15	0.005	99.07
	2097	0.059	24.33	0.019	0.021	37.83	23.71	0.066	0.012	13.20	0.010	99.25
	2097	0.028	23.89	0.018	0.107	37.87	24.97	0.592	0.067	11.67	0.001	99.21
	2097	0.069	24.15	0.000	0.095	38.12	24.03	0.436	0.027	12.14	0.004	99.06
	2097	0.018	24.17	0.000	0.058	37.53	23.25	0.188	0.024	13.80	0.000	99.04
	2097	0.107	24.73	0.004	0.055	38.30	26.77	0.038	0.000	9.66	0.002	99.67
	2097	0.028	22.94	0.427	0.157	38.84	25.07	0.304	0.045	11.55	0.010	99.37
	2199	0.101	23.99	0.007	0.032	37.80	24.44	0.511	0.000	11.97	0.007	98.86
	2199	0.085	23.83	0.000	0.016	38.13	25.06	0.462	0.000	12.20	0.004	99.78
	2199	0.139	24.08	0.013	0.056	38.01	23.51	0.268	0.000	13.15	0.001	99.23
	2199	0.025	23.84	0.033	0.047	37.99	25.38	0.354	0.000	11.23	0.009	98.90
	2199	0.364	23.93	0.012	0.107	37.25	21.35	0.155	0.012	15.46	0.000	98.64
	2199	0.124	23.80	0.011	0.087	37.87	26.26	1.057	0.021	9.55	0.002	98.79
	2199	0.030	24.05	0.003	0.019	38.05	25.19	0.427	0.000	11.29	0.000	99.06
	2298	0.034	23.68	0.010	0.072	37.70	22.76	0.118	0.000	12.40	0.000	96.77
	2298	0.015	24.22	0.017	0.043	38.13	25.45	0.351	0.033	11.20	0.001	99.46

PAL30D (cont'd)	2395	0.007	24.32	0.000	0.016	38.09	24.79	0.122	0.015	12.15	0.003	99.52
	2395	0.103	23.69	0.001	0.051	37.55	22.12	0.188	0.000	14.97	0.006	98.67
	2395	0.008	24.25	0.001	0.020	37.84	24.66	0.104	0.000	11.49	0.000	98.37
	2395	0.011	21.94	0.002	1.202	37.75	21.09	0.228	0.018	15.04	0.122	97.37
	2395	0.003	23.87	0.000	0.059	37.48	21.21	0.108	0.042	16.05	0.000	98.82
	2395	0.000	23.28	0.000	0.072	37.71	22.60	0.479	0.036	14.61	0.006	98.78
	2395	0.000	23.66	0.003	0.022	36.84	19.36	0.014	0.000	18.58	0.005	98.47
	2395	0.017	23.45	0.031	1.329	38.97	24.55	0.101	0.000	10.27	0.006	98.72
	2395	0.010	24.00	0.173	0.038	38.28	23.43	0.099	0.000	13.32	0.004	99.36

PAL8RD (cont'd)	2298	0.020	26.43	0.016	0.111	35.41	24.27	0.184	0.058	10.05	0.014	96.56
	2298	0.005	24.10	0.000	0.081	37.71	22.59	0.359	0.000	14.55	0.000	99.39
	2298	0.022	24.14	0.015	0.027	37.99	23.88	0.360	0.015	13.39	0.001	99.83
	2298	0.085	24.26	0.008	0.041	37.83	24.52	0.071	0.006	12.10	0.002	98.93
	2388	0.099	23.84	0.000	0.062	37.25	20.46	0.109	0.006	16.79	0.000	98.61
	2388	0.027	24.12	0.014	0.131	37.99	24.58	0.218	0.015	11.38	0.003	98.48
	2388	0.008	23.45	0.030	0.106	37.69	24.13	0.493	0.033	12.60	0.002	98.55
	2388	0.036	24.27	0.014	0.042	38.09	26.16	0.100	0.000	10.21	0.003	98.92
	2388	0.093	24.48	0.001	0.051	38.00	25.25	0.119	0.012	11.20	0.004	99.21
	2388	0.069	24.08	0.000	0.024	37.73	24.04	0.147	0.034	12.39	0.007	98.53
	2388	0.291	23.06	0.004	0.146	35.38	21.26	0.304	0.006	18.82	0.003	99.27
	2690	0.039	23.40	0.013	0.044	37.83	26.18	0.965	0.000	9.70	0.002	98.17
	2690	0.035	22.92	0.005	0.047	37.60	26.25	0.850	0.030	10.11	0.001	97.85
	2690	0.021	24.18	0.000	0.005	38.05	25.02	0.239	0.058	11.59	0.000	99.16
	2690	0.142	24.41	0.000	0.030	37.96	25.75	0.183	0.000	10.75	0.000	99.21
	2690	0.049	24.05	0.002	0.015	37.81	24.89	0.218	0.052	11.68	0.000	98.77
	2690	0.021	23.80	0.000	0.029	37.77	25.62	0.429	0.021	11.04	0.002	98.73

Sample depths are in meters, measured depth (mMD). n.d. – not detected. Total Fe expressed as FeO.

~~Supplementary~~ Supplemental Table 2: Normalized major and trace element concentrations obtained through X-ray fluorescence analysis of samples from well PAL8RD.

Depth mMD	Al_2O_3	CaO	Fe_2O_3	K_2O	MgO	MnO	Na_2O	P_2O5	SiO_2	TiO_2
	Major elements									
	Weight Percent									
1998	18.96	7.81	9.24	2.15	3.66	0.16	3.05	0.49	53.02	1.01
2097	19.62	8.68	8.85	1.28	2.17	0.17	3.85	0.46	53.61	0.92
2199	20.33	8.85	7.85	1.14	2.04	0.16	4.24	0.47	53.56	0.91
2298	19.28	9.10	8.80	1.16	2.72	0.17	3.24	0.44	53.79	0.91
2388	19.45	9.99	9.65	1.25	4.05	0.14	2.88	0.37	50.90	0.97
2690	16.26	16.27	7.22	1.53	2.05	0.17	1.34	0.34	51.30	0.67

Depth mMD	As	Ba	Ce	Cr	Cs	Cu	Ga	La	Nd	Pb	Rb	S	Sc	Sr	Th	V	Y	Zn
	Trace elements																	
	ppm																	
1998	42	549	55	53	12	93	20	41	26	7	47	1959	35	868	10	203	20	89
2097	4	446	54	40	9	127	20	33	18	9	18	1455	31	1058	9	250	22	90
2199	3	412	37	30	5	85	20	34	14	7	17	1988	19	1150	8	226	20	88
2298	3	445	39	47	16	256	19	22	18	9	16	1207	16	1210	7	264	20	116
2388	25	533	52	56	-	116	20	24	18	5	16	734	38	1223	11	310	17	81
2690	1	501	36	9	-	1277	21	17	-	2280	17	18803	21	1571	3	230	18	3531

~~Supplementary~~ Supplemental Table 3: Updated representative chemistry of well discharge fluids from Bacman wells.

Well	Sampling date yymmdd	Enthalpy kJ/kg	Sampling pressure MPa (absolute)	pH at 25°C	Li	Na	K	Ca	Mg	Fe	Cl	SiO_2	B	SO_4	HCO_3	NH_3	H_2S	CO_2 total	Cl_{res}	T_{quartz}* °C	Cl/B
					mg/kg																
PAL3D	160202	1245	0.860	7.00	7.08	4631	807	259	0.42	0.16	8011	638	35.2	20.2	16.9	4.07	1.67	17.6	6749	244	71
PAL4D	160215	1328	1.160	7.10	7.76	4727	843	259	0.46	0.11	8112	688	36.5	17.4	-	4.49	2.92	0.2	6924	249	70
PAL8D	160203	1440	0.990	6.60	8.76	5603	1033	242	0.40	0.12	9679	706	52.9	14.5	40.8	9.91	4.53	50.8	8083	251	57
PAL9D	160202	1440	0.990	6.70	8.12	4521	870	206	0.51	-	7893	691	32.9	22.2	13.4	5.69	1.78	17.5	6624	250	75
PAL10D	160215	2022	0.940	6.90	9.33	4979	1099	206	0.46	0.42	8754	738	46.6	35.9	82.0	26.50	7.63	77.3	7199	255	59
PAL11D	160209	2493	0.960	6.60	7.66	5447	856	474	0.92	0.21	9755	370	55.7	49.9	52.8	22.20	7.16	57.4	9170	205	55
PAL12D	160201	1300	1.930	7.10	8.45	5454	971	285	0.52	0.06	9421	668	48.0	18.3	32.2	6.98	2.62	30.8	8569	247	62
PAL13D	160217	1404	0.940	7.10	6.14	3955	665	254	0.48	0.05	7007	551	31.0	27.0	18.0	5.00	1.50	19.0	6134	233	71
PAL14D	160201	1292	1.000	7.10	7.52	5125	952	237	0.63	0.05	9211	697	50.2	31.3	21.7	6.07	2.11	21.5	7722	250	58
PAL15D	160123	1524	0.990	6.70	7.46	4641	885	236	0.39	0.13	7992	663	39.6	25.9	-	14.60	2.61	5.3	6769	247	63
PAL18D	160205	1200	0.96	6.70	8.28	5298	808	270	0.71	0.10	9521	617	53.5	29.0	48.1	9.14	2.64	52.0	8163	241	56
PAL19	160210	1492	0.980	6.70	8.70	5810	1042	300	0.63	-	9764	757	49.9	21.8	19.9	6.71	2.69	22.0	8014	257	61
PAL20D	160205	1708	1.090	6.50	13.80	6071	1441	272	0.29	0.06	11568	747	111.0	14.0	20.5	15.20	7.64	37.8	9628	256	33
PAL21	160217	1093	0.910	6.20	6.64	4205	716	294	0.46	0.25	7760	602	34.0	20.9	27.0	3.44	1.64	41.2	6653	239	72
PAL22D	151028	1082	0.890	7.10	6.44	4072	665	258	0.32	0.13	7011	597	30.4	29.3	13.9	3.64	1.20	14.0	6009	239	72
PAL23D	160203	1171	0.920	6.60	9.61	5456	988	216	0.44	0.09	9578	736	53.6	16.0	30.9	5.26	2.62	34.7	7866	255	56
PAL25D	160223	1084	0.980	6.50	7.36	4685	819	262	0.37	0.86	8272	625	35.9	25.6	22.4	3.64	2.49	29.5	7088	242	72
PAL26D	160219	1446	1.060	6.40	13.90	5608	1456	206	0.54	0.27	10344	1031	67.5	8.2	40.5	12.70	5.00	52.2	7874	283	48
PAL27D	160216	1481	1.230	6.90	9.33	4757	1059	178	0.41	-	8476	786	44.3	16.1	108.0	28.30	12.00	99.1	7056	260	60
PAL28D	160222	1053	0.870	6.90	6.85	4635	791	272	0.24	0.10	8034	644	34.1	19.8	21.8	3.25	1.87	22.2	6762	244	74
PAL30D	160222	1241	1.07	6.70	7.56	4329	855	202	0.26	-	7666	755	30.5	17.9	22.6	4.09	2.02	25.3	6352	257	79
OP3D	090218	1963	0.820	7.32	20.50	0	1727	234	0.00	0.00	11962	987	145.0	11.0	114.0	0.00	158.00	105.0	8993	279	26
OP4D	090302	2124	0.845	6.43	15.70	6473	1698	224	0.13	0.03	12334	909	129.0	15.4	107.0	5.52	10.40	122.0	9521	272	30
OP5DA	090414	1917	0.700	6.83	11.90	2905	740	127	0.00	0.00	5441	343	109.0	12.4	0.0	13.40	9.93	61.9	5028	200	16
OP6D	091009	2279	0.700	6.86	0.10	27	5	8.32	0.08	0.12	3603	46	353.0	15.5	461.0	2.53	29.90	423.0	4094	99	3
OP7D	090302	2081	0.755	7.99	13.60	5760	1396	257	0.10	0.42	10659	797	81.7	11.4	15.0	6.42	6.96	4.0	8427	261	41
CN1	130702	1316	1.120	5.24	8.94	4655	748	145	3.50	3.63	8355	796	34.8	81.6	16.3	25.60	1.76	40.4	6866	261	75
CN3D	160219	1905	0.700	5.60	1.69	1513	213	26	15.80	21.60	1822	439	13.6	1252.0	-	189.00	0.80	3.2	1618	217	42
CN4D	160122	1273	0.730	7.10	7.72	4442	808	227	0.47	0.15	7644	681	33.5	18.8	16.3	6.41	1.19	15.1	6253	249	72
CN5D	160122	1290	0.800	6.90	8.31	4748	911	246	0.88	0.38	8641	686	37.7	20.2	3.2	7.66	1.41	4.6	7117	249	72
RS1D	150604	2381	0.32	6.18	6.75	2395	756	126	0.58	1.39	4468	685	233.0	60.6	310.0	88.60	196.00	232.0	3410	249	6
TW1D	130521	1296	0.9	7.52	9.34	4115	962	213	0.31	0.09	7612	709	30.1	17.2	21.3	7.42	2.06	38.6	6292	252	79
TW2D	121003	1267	0.094	7.90	9.25	5099	1028	226	0.31	0.25	9107	790	42.6	20.8	16.7	8.85	1.74	28.7	6181	260	67
TW4D	130521	1291	0.92	6.90	9.01	3975	805	222	0.26	0.12	6948	662	32.0	23.9	40.5	9.49	2.80	57.3	5844	246	68

* Reservoir fluid temperatures were calculated using the quartz geothermometer (T_{quartz}) considering maximum steam loss by Fournier (1977).
Well code: PAL for wells found in Palayang Bayan sector; OP for wells in Botong sector; CN for wells in Cawayan sector; RS for the well in Rangas sector; and TW for wells in Tanawon sector.

~~Supplementary~~ Supplemental Table 4: Updated chemistry and isotopic analysis in total discharge (TD) and reservoir (res) conditions of discharge fluid and steam condensate samples from Bacman wells.

Well	Sampling date	Sampling pressure	Enthalpy (H)	T_{quartz}*	H at T_{quartz}	Excess H (H-H T_{quartz})	δD liquid	δD steam condensate	$\delta^{18}O$ liquid	$\delta^{18}O$ steam condensate	Cl	δD TD	$\delta^{18}O$ TD	Cl TD	Fractionation factor at T_{quartz}		δD_{res}	$\delta^{18}O_{res}$	Cl_{res}
	yymmdd	MPa (absolute)	kJ/kg	°C	kJ/kg	kJ/kg	‰				mg/kg	‰		mg/kg	$10^3 \ln\alpha\ D_{l-v}$	$10^3 \ln\alpha\ ^{18}O_{l-v}$	‰		mg/kg
CN1	121011	0.65	1149	180	763	386	-22.6	-25.1	-3.75	-4.19	2110	-23.2	-3.85	473	6.5	2.78	-21.9	-3.32	-
CN3D	150611	0.70	2349	241	1042	1307	-18.0	-18.5	-1.22	-2.06		-18.4	-1.89		-1.1	1.64	-19.2	-0.67	-
CN4D	150611	0.78	1273	261	1140	133	-19.2	-22.4	-1.50	-3.66	8373	-20.1	-2.09	2271	-2.4	1.34	-20.3	-1.98	6645
CN5D	150618	0.77	1290	265	1160	130	-18.0	-22.0	-1.45	-3.69	8712	-19.1	-2.08	2446	-2.6	1.28	-19.3	-1.98	6818
OP3D	090218	0.82	1963	303	1362	601	-18.1	-19.3	4.14	1.61	11962	-18.9	2.61	7246	-3.6	0.78	-20.4	2.95	8235
OP4D	090219	0.83	2124	300	1345	779	-16.8	-23.3	2.68	-0.45	12055	-21.2	0.54	8246	-3.6	0.81	-23.2	0.99	8409
PAL3D	150606	0.92	1245	263	1150	95	-19.1	-22.9	-2.10	-4.43	7937	-20.0	-2.67	1951	-2.5	1.31	-20.2	-2.60	6359
PAL4D	150624	1.06	1230	270	1185	45	-19.3	-23.5	-1.86	-4.34	8078	-20.3	-2.42	1839	-2.9	1.21	-20.3	-2.39	6420
PAL8D	150615	1.05	1561	271	1190	371	-17.5	-21.0	0.01	-2.41	9898	-18.9	-0.94	3895	-2.9	1.20	-19.5	-0.66	7831
PAL9D	150615	0.88	1296	269	1180	116	-18.9	-21.9	-1.86	-3.99	8083	-19.7	-2.44	2218	-2.8	1.23	-19.9	-2.36	6326
PAL10D	150610	0.92	2029	276	1216	813	-18.6	-15.4	0.42	-0.64	9327	-16.6	-0.25	5902	-3.1	1.13	-18.2	0.33	7168
PAL11D	150909	0.91	2675	223	958	1717	-13.7	-19.0	0.12	-2.53	8831	-18.7	-2.40	8406	0.6	1.94	-18.2	-0.59	7904
PAL12D	150602	0.92	1299	269	1180	119	-21.8	-17.0	-3.21	-0.56	9841	-20.5	-2.49	2681	-2.8	1.23	-20.7	-2.40	7738
PAL13D	150609	0.96	1409	258	1125	284	-18.4	-21.8	-1.37	-3.75	8181	-19.5	-2.14	2649	-2.3	1.38	-19.9	-1.91	6683
PAL14D	150602	1.05	1221	274	1206	15	-17.9	-20.7	-0.44	-2.72	9959	-18.5	-0.95	2232	-3.0	1.16	-18.6	-0.94	7803
PAL15D	150609	0.95	1522	264	1155	367	-18.1	-22.4	-0.76	-3.35	8177	-19.7	-1.75	3113	-2.6	1.30	-20.3	-1.46	6549
PAL18D	150603	0.95	1155	253	1100	55	-17.9	-22.3	-0.49	-3.02	8999	-18.8	-0.99	1791	-2.0	1.46	-18.9	-0.95	7451
PAL19	150603	0.96	1526	274	1206	320	-18.0	-18.3	-1.32	-3.10	9687	-18.1	-2.00	3697	-3.0	1.16	-18.7	-1.77	7527
PAL20D	150909	1.04	1708	277	1221	487	-18.5	-22.3	1.33	-1.23	11490	-20.3	0.13	5368	-3.1	1.11	-21.3	0.48	8908
PAL22D	150623	0.98	1188	257	1120	68	-19.1	-23.0	-2.02	-4.52	7406	-19.9	-2.55	1579	-2.2	1.40	-20.0	-2.50	6077
PAL23D	150606	0.85	1095	273	1201	-106	-17.3	-22.0	-0.43	-3.25	9930	-18.1	-0.93	1766	-3.0	1.17	-17.9	-1.01	7650
PAL25D	150617	1.05	1181	256	1115	66	-18.9	-21.8	-1.94	-4.05	7523	-19.5	-2.37	1537	-2.2	1.41	-19.5	-2.32	6233
PAL26D	150610	1.03	1450	309	1397	53	-18.8	-17.9	0.37	-1.24	10287	-18.5	-0.18	3490	-3.6	0.70	-18.7	-0.15	7071
PAL27D	150624	1.03	1479	283	1253	226	-18.7	-22.2	-0.25	-2.90	8453	-20.0	-1.19	2990	-3.3	1.03	-20.5	-1.03	6416
PAL30D	150615	1.03	1241	276	1216	25	-20.3	-23.2	-1.89	-4.12	7649	-21.0	-2.41	1799	-3.1	1.13	-21.0	-2.40	5945
RS1D	150331	0.77	2098	289	1285	813	-17.8	-23.4	8.44	5.83	-	-21.6	6.68	-	-3.5	0.95	-23.5	7.20	-

* Reservoir fluid temperatures were calculated using the quartz geothermometer (T_{quartz}) considering maximum steam loss by Fournier (1977). Fractionation factors between liquid (l) and steam (v) at T_{quartz} for both D/H and $^{18}O/^{16}O$ were based on equations by Horita and Wesolowski (1994).